

Distinguishability and Chiral Stability: Effects of Decoherence and Intermolecular Interactions

Heekyung Han^{1,*} and David M. Wardlaw^{1,2,†}

¹*Department of Chemistry, Queens University, Kingston, Ontario K7L , Canada*

²*Department of Chemistry, University of Western Ontario,
London, Ontario N6H 5B7, Canada*

(Dated: October 20, 2018)

Abstract

We examine the effect of decoherence and intermolecular interactions (chiral discrimination energies) on the chiral stability and the distinguishability of initially pure versus mixed states in an open chiral system. Under a two-level approximation for a system, intermolecular interactions are introduced by a mean-field theory, and interaction between a system and an environment is modeled by a continuous measurement of a population difference between the two chiral states. The resultant equations are explored for various parameters, with emphasis on the combined effects of the initial condition of the system, the chiral discrimination energy and the decoherence. We focus on factors affecting the distinguishability as measured by population difference between the initially pure and mixed states and on the chiral stability as measured by the purity decay.

*E-mail address: hhan0410@gmail.com

†E-mail address: dwardlaw@uwo.ca

I. INTRODUCTION

The existence of stable chiral molecules has been one of the most puzzling problems in quantum mechanics [1]. Since the Hamiltonian of chiral molecules is symmetric with respect to the parity operation, the eigenfunctions of the parity-invariant Hamiltonian should also be parity eigenfunctions in the absence of energy degeneracy [2], i.e., the left- and right-handed states of chiral molecules are not true stationary states. However, some enantiomers are observed to be stable for a remarkably long time despite their lack of parity symmetry. In the early days of quantum-mechanics Hund formulated the problem of the stability of chiral molecules in terms of quantum tunneling in a symmetrical double-well potential [1]. The two chiral states are represented by coherent superposition of the eigenstates. When only the lowest two eigenstates, $|+\rangle$ (even parity, ground) and $|-\rangle$ (odd parity) with energies E_+ and E_- , are relevant in a description of the system, the two chiral states, $|L\rangle$ and $|R\rangle$, localized around the potential minima, may be written as

$$|L\rangle = \frac{1}{\sqrt{2}}(|+\rangle + |-\rangle), \quad (1)$$

$$|R\rangle = \frac{1}{\sqrt{2}}(|+\rangle - |-\rangle). \quad (2)$$

Hence, if the system is initially prepared as one of the two chiral states, say, $|R\rangle$, it will oscillate between $|R\rangle$ and $|L\rangle$ through the inter-well barrier. The tunneling time is inversely proportional to the energy splitting between the two lowest eigenstates. An exceedingly long tunneling time corresponding to an extremely small energy splitting was thought to be responsible for the stability of chirality. However, upon a quantitative test, Hund's theory seems rather insufficient since the tunneling times observed for stable chiral molecules vary in a wide range, from sub-picosecond to the age of the universe, depending on the mass of the particle and the nature of the potential, and yet no quantum tunnelings are observed in these molecules. Interest in the paradox of chiral stability was redrawn by the discovery of weak neutral currents which violate parity symmetry at the level of nonrelativistic quantum mechanics, and thus may lead to stabilization of one of the two chiral configurations. However, while theoretical calculations for this effect predict smaller energies of predominant (L)-amino-acids and (D)-sugars than their corresponding enantiomers, the energy difference is too small to be detected experimentally so far [3]. On the other hand, some have noted that a nonlinear Schrödinger equation does not require the eigenstates of the potential's

symmetry operators as the stationary states [4]. More recently, Vardi showed that the effect of a difference between homochiral interactions (the intermolecular interactions between molecules of the same chirality) and heterochiral interactions (the intermolecular interactions between molecules of the opposite chirality), due to resultant nonlinearity of equations, can lead to far more stabilized chiral states than expected for isolated molecules [5]. Several authors also have pointed out that the interaction of molecules with the environment should be introduced to explain the stability of chiral molecules. The environmental effects on the system leads to decoherence, i.e. , coherence loss, and thus to a suppression of coherent tunneling oscillations. Intermolecular collisions [6], interaction with photons [7], and interaction with phonons [8] have also been employed as the origin of the dephasing process. Another problem related to the issue of stabilization of chiral molecules is controlling the chirality by exploiting lasers: several proposals have been suggested for the preparation and detection of the superposed chiral states utilizing phase-controlled ultrashort laser pulses [9], and growing attention has been directed towards using lasers to manipulate the molecular chirality [10]. Considering that effects of the decoherence and the intermolecular interactions on the system and thus on the control scenarios are far from well-understood despite their expected serious impacts, it is thus of great interest to understand the coherent tunneling dynamics of chiral systems coupled to external environments more thoroughly. In the related work [11], we considered an open chiral system, where a two-level approximation was taken for the system, and interaction between a system and an environment was modeled by a continuous position measurement, an approach often used in the studies of the quantum Zeno effect [12] and in the studies of decoherence effects in chemical reactions [13]. In particular, we focused on the interplay of the initial coherences and the decoherence on the distinguishability of initially pure versus initially mixed states as measured by a population difference between the two chiral states, and on the vulnerability to decoherence as measured by a purity decay. The results provided some answers to three fundamental questions arising in open chiral systems as follows. 1) Can we distinguish a pure state from a mixture with same populations as those of the pure state? If the two chiral states are initially taken to be real for the pure state, no distinguishability was shown to exist for all time and any dephasing rate. Otherwise, the distinguishability exists, although it disappears over time faster with increasing the dephasing rate. 2) Why are some chiral systems stable for a very long time? 3) Why are superpositions of stable chiral states not observed experimentally? Our result

suggested that the system, if it is initially a well-localized state, would tend to preserve its chirality when coupled to an environment that destroys left-right coherences, provided that the interaction time scale (dephasing time) is faster than the tunneling time scale. On the other hand, the system, if initially a superposition of two chiral states, would become very quickly a racemic mixture in the presence of the very same environment. In this paper, we extend the open chiral system considered in Ref. [11] to include chiral intermolecular interactions which are introduced within a mean-field approximation as used in Ref. [5]. To better understand the combined effects of the two interactions, namely the decoherence effect and chiral intermolecular interactions, we first consider the system in the presence of each interaction separately, review some results of Ref. [5], [11], and then further obtain the following results. 1) For a system with decoherence only and with an initially localized state, decreasing the tunneling frequency tends to suppress the decoherence process. It suggests that the more classical system is less vulnerable to decoherence. 2) For a system with chiral intermolecular interactions only, the nonzero chiral discrimination energies can bring about the distinguishability between the initially pure and the mixed states even when the chiral states are taken to be real for the initially pure state, where no distinguishability exists in the absence of chiral intermolecular interactions. It makes it clear that Vardi's claim in the Ref. [5] (“... *In the former case, spontaneous symmetry breaking may take place, turning a nearly racemic mixture into an optically active ensemble*”), is unjustifiable since he used initially pure states without any decoherence source, and thus initially pure states should remain pure, and initially pure state and mixed state are shown to behave differently in the presence of intermolecular interactions. Finally, we introduce both the decoherence and chiral intermolecular interactions into our model system. The dephasing time is varied to be very long compared with tunneling time. In this tunneling dominant region, the decoherence process in the absence of chiral intermolecular interactions is very slow, but, however, when combined with the chiral intermolecular interactions, the decoherence process tends to be accelerated. For a given chiral discrimination energy, we observe that, similar to the case with decoherence only, as the dephasing rate increases, the decoherence process becomes faster. On the other hand, for a given dephasing rate, the decoherence process is seen to be influenced by the initial condition of the system and the chiral discrimination energy. That is, the vulnerability of the system to decoherence depends on whether the initial state is strongly delocalized or localized, and whether chiral discrimination energy favors homochiral

mixtures or heterochiral mixtures. The organization of this work is as follows. Section II presents formulations of a chiral system in the presence of intermolecular interactions and decoherence effects. Section III gives brief descriptions of the initial conditions, measures of the distinguishability and the coherence loss, and computational methods. In Sec. IV the system in the presence of decoherence only is examined with a particular focus on how the initial coherence, dephasing rate, and tunneling frequency affect the distinguishability and the purity decay. In Sec. V the system in the presence of intermolecular interactions only is examined with an emphasis on the distinguishability of the initially pure and mixed states, as afforded by the intermolecular interactions. In Sec. VI both effects, the decoherence and the intermolecular interactions are introduced, and the combined effects are examined on the purity decay rate and the stationary values of the population and the coherence, with several different initial states for the system. Finally, Sec. VII provides conclusions and discuss further studies.

II. FORMULATION: CHIRAL SYSTEMS IN THE PRESENCE OF DEPHASING AND INTERMOLECULAR INTERACTIONS

To study the behavior of chiral molecules we adopt the framework of Hund's double-well model [1]: the chiral molecule is characterized by a symmetric, one-dimensional double-well potential $V(x)$ and the x coordinate corresponds to the chiral configuration. Also we take a two-level approximation for the system, i.e., consider only the two lowest energy eigenstates, this is valid when the energy is sufficiently low that other higher energy eigenstates are not involved in the system dynamics. The total wavefunction of the system may be written as

$$|\Psi(t)\rangle = a_L(t)|L\rangle + a_R(t)|R\rangle, \quad (3)$$

The Hamiltonian for an isolated system in the two-level approximation takes the form

$$\hat{H}_0 = E_+|+\rangle\langle+| + E_-|-\rangle\langle-|, \quad (4)$$

$$= E_m(|R\rangle\langle R| + |L\rangle\langle L|) - \delta(|L\rangle\langle R| + |R\rangle\langle L|) \quad (5)$$

where $E_m = \frac{(E_+ + E_-)}{2}$ and $\delta = \frac{(E_- - E_+)}{2} \equiv \hbar\omega$, where ω is the tunneling frequency. Substitution of Eq.(5) into the time-dependent Schrödinger equation $i\hbar\frac{\partial}{\partial t}|\Psi\rangle = \hat{H}_0|\Psi\rangle$ leads to a set

of two linear equations for the expansion coefficients a_R and a_L :

$$i\hbar\dot{a}_L = E_m a_R - \delta a_L, \quad (6)$$

$$i\hbar\dot{a}_R = E_m a_L - \delta a_R. \quad (7)$$

The time evolution of a_R and a_L shows a tunneling motion of the system between the two wells with oscillation frequency ω . Note that the tunneling time ($= 2\pi/\omega = 2\pi\hbar/\delta$) is inversely proportional to the energy difference between the states $|+\rangle$ and $|-\rangle$. To take into account the effect of the intermolecular interactions, in particular, the homochiral interactions and the heterochiral interactions, we choose Vardi's approach [5]. In Ref. [5] he employs a Hartree-Fock technique, where each molecule sees only the mean field that is generated by the interactions of all the other molecules. The homochiral and the heterochiral interactions lead to two components of the self-consistent field, V_{hom} and V_{het} , respectively. Then, Eqs. (6), (7) become

$$\dot{a}_L = -\frac{i}{\hbar}(E_m a_L - \delta a_R) - \frac{i}{\hbar}(V_{hom}|a_L|^2 + V_{het}|a_R|^2) a_L, \quad (8)$$

$$\dot{a}_R = -\frac{i}{\hbar}(E_m a_R - \delta a_L) - \frac{i}{\hbar}(V_{hom}|a_R|^2 + V_{het}|a_L|^2) a_R. \quad (9)$$

Here, the time-evolution is governed by two terms. The first comes from the dynamics of the isolated system which generates a coherent tunneling between two wells. The second term involving V_{hom} and V_{het} is responsible for the intermolecular (hetero/homochiral) interactions between the single molecule with the other surrounding molecules within the mean-field approximation [5]. Note that introducing the intermolecular interactions results in a nonlinear Schrödinger equation of which the stationary states does not need to be eigenstates of the parity operator [4]. Vardi showed that if V_{hom} and V_{het} are different, the second term involving nonlinear terms may affect the equation of motion significantly, and can lead to more stabilized chiral states or achiral states than expected for the corresponding isolated molecule, depending on the initial condition and the difference between V_{hom} and V_{het} [5]. However, in the mean field approximation fluctuation terms are ignored. These fluctuation terms arise from the interaction between molecules and are expected to result in decoherence. Thus, in Ref. [5] the system does not go through coherence loss and never becomes a mixed state when starting from a pure state. Below we combine the intermolecular interactions and the decoherence effect to describe the dynamics of chiral molecules. In order to simulate the decoherence effect, we consider the environment surrounding the system: the

environment can be thought of as other degrees of freedom of the system or an inert gas or a condensed phase of no chirality. We model the effects of interactions between the system and the environment as the continuous measurement of the system coordinate \hat{x} [14, 15]. Then the system density operator $\hat{\rho}$, which is obtained by tracing the total density operator over the environment, obeys the master equation [13],

$$\frac{\partial \hat{\rho}}{\partial t} = -\frac{i}{\hbar}[\hat{H}, \hat{\rho}] - \gamma'[\hat{x}, [\hat{x}, \hat{\rho}]], \quad (10)$$

with γ' being a coupling strength between the system and the environment. The first term represents the system dynamics in the absence of the environment, and the second term, a multiplication of γ' and the double commutator, is responsible for the environmental effect on the system and is expected to destroy coherences between the eigenstates of the position measurement operator, \hat{x} . This loss of coherence, i.e., decoherence, has been argued as the essential ingredient to reconcile the two conflicting descriptions of chiral stability, the classical “localized” one and the quantum “delocalized” one [12, 16]. To invoke a two-level approximation for the system, we assumed that the potential barrier is very high, or equivalently the energy of the system is sufficiently low that the higher energy levels are not involved in the dynamics. In addition, since we introduced the environment, we should point out that the position measurement of the system is known to increase both its energy $\langle \hat{H} \rangle$ and energy width $\delta E \equiv \sqrt{\langle \hat{H}^2 \rangle - \langle \hat{H} \rangle^2}$, where $\langle \cdot \rangle$ denotes an ensemble-average, over time [13, 17]. The system energy and energy width will eventually become greater than the next higher energy levels, leading to the breakdown in the validity of the two-level approximation. The stronger γ' , the shorter the time during which the two-level approximation will be valid. Using the two-level approximation and the evenness of $|+\rangle$ and oddness of $|-\rangle$, we derive the position measurement operator as

$$\begin{aligned} \hat{x} &\approx |+\rangle\langle +|\hat{x}|-\rangle\langle -| + \text{H.c} \\ &= x_{\text{avg}}\hat{\sigma}_z \approx x_{\text{min}}\hat{\sigma}_z, \end{aligned} \quad (11)$$

where H.c denotes the Hermitian conjugate and $\hat{\sigma}_z \equiv (|R\rangle\langle R| - |L\rangle\langle L|)$. Here $\pm x_{\text{min}}$ are the positions of the double-well minima, which for a deep well are very close to the average positions of the right and left wave functions (denoted by $\pm x_{\text{avg}}$ with definitions $x_{\text{avg}} \equiv \langle R|\hat{x}|R\rangle$ and $-x_{\text{avg}} \equiv \langle L|\hat{x}|L\rangle$). Then the master equation for the two-level system becomes

[18]

$$\frac{\partial \hat{\rho}}{\partial t} = \frac{i}{\hbar} [\hat{H}, \hat{\rho}] - \gamma [\hat{\sigma}_z, [\hat{\sigma}_z, \hat{\rho}]], \quad (12)$$

with the dephasing rate $\gamma \equiv \gamma' x_{\min}^2$. This equation gives the evolution of the two-level system subjected to $\hat{\sigma}_z$ representing a continual measurement of the system coordinate \hat{x} . In the first term we will use the Hamiltonian of the two-level system with the intermolecular interactions under a mean-field approximation as used in Eqs. (8) and (9). The second term in this equation represents a measurement of a population difference between two states $|L\rangle$ and $|R\rangle$, and leads to decay of the coherences between the $|L\rangle$ and $|R\rangle$ states (decay of the off-diagonal matrix elements, ρ_{LR}). To amalgamate Eqs. (8), (9) and Eq. (12), we rewrite Eq. (12) into the stochastic Schrödinger equation for the state vector $|\Psi\rangle$ [18, 19]:

$$|d\Psi\rangle = \left(-\frac{i}{\hbar} \hat{H} - \gamma [\hat{\sigma}_z - \langle \hat{\sigma}_z \rangle_{|\Psi\rangle}]^2 \right) |\Psi\rangle dt + \sqrt{\gamma} [\hat{\sigma}_z - \langle \hat{\sigma}_z \rangle_{|\Psi\rangle}] |\Psi\rangle d\xi, \quad (13)$$

where $\langle \hat{\sigma}_z \rangle_{|\Psi\rangle} = \langle \Psi | \hat{\sigma}_z | \Psi \rangle$ and ξ is for a complex Wiener process [19]. Combining the intermolecular interactions and the decoherence leads to the resultant Schrödinger equation in terms of a_L and a_R , which is stochastic and nonlinear:

$$\dot{a}_L = -\frac{i}{\hbar} (E_m a_L - \delta a_R) - \frac{i}{\hbar} (V_{hom} |a_L|^2 + V_{het} |a_R|^2) a_L - \left(\gamma |a_R|^4 + \sqrt{\gamma} \dot{\xi}(t) |a_R|^2 \right) a_L \quad (14)$$

$$\dot{a}_R = -\frac{i}{\hbar} (E_m a_R - \delta a_L) - \frac{i}{\hbar} (V_{hom} |a_R|^2 + V_{het} |a_L|^2) a_R - \left(\gamma |a_L|^4 - \sqrt{\gamma} \dot{\xi}(t) |a_L|^2 \right) a_R \quad (15)$$

Here, the time-evolution is governed by three components. The first and the second components are responsible for the dynamics of the isolated system and for the intermolecular (hetero/homochiral) interactions between the single molecule with the other surrounding molecules within the mean-field approximation [5], respectively. The last component models the interaction with the environment that induces the loss of quantum coherence in the system. Noting that $|a_R|^2 + |a_L|^2 = 1$, and rescaling the time as $\omega t \rightarrow t$, Eqs. (14) and (15) become

$$\dot{a}_L = -i (\Omega + v |a_R|^2) a_L + i a_R - \left(\Gamma |a_R|^4 + \sqrt{\Gamma} \dot{\eta}(t) |a_R|^2 \right) a_L, \quad (16)$$

$$\dot{a}_R = -i (\Omega + v |a_L|^2) a_R + i a_L - \left(\Gamma |a_L|^4 - \sqrt{\Gamma} \dot{\eta}(t) |a_L|^2 \right) a_R, \quad (17)$$

with $\Omega = (E_m + V_{hom})/\delta$, $v = (V_{het} - V_{hom})/\delta$, $\Gamma = \gamma/\omega$ and $d\eta = \sqrt{\omega} d\xi$. We gradually build up a more complicated system starting from a simple system. In section IV we study

the system in the presence of decoherence effect only, using Eq. (12) with $\hat{H} = \hat{H}_0$ where \hat{H}_0 is given in Eq.(5). In section V we study the system in the presence of intermolecular interactions only, using Eqs.(8) and (9). In section VI, we study the system in the presence of the combined effects of the decoherence and the intermolecular interactions, using Eqs.(16) and (17).

III. THE MODEL

A. Initial condition: Localized and delocalized states

We examine three cases for the pure state with an initially different coherence, or equivalently with an initially different degree of localization. For an initially localized state (denoted as LS), we choose $|R\rangle$, located in the right-well. For an initially delocalized state, we examine two cases, a weakly delocalized state (denoted as WDS) and a strongly delocalized state (denoted as SDS), with $\sqrt{0.05}|L\rangle + \sqrt{0.95}|R\rangle$ and $\sqrt{0.49}|L\rangle + \sqrt{0.51}|R\rangle$, respectively. For the LS case, the initial coherence ($\equiv \rho_{LR}$) is 0, and the initial population difference between the two chiral states, Z ($\equiv \rho_{RR} - \rho_{LL}$) is 1. For the WDS case, initially $\rho_{LR} = \sqrt{0.05 \times 0.95} \approx 0.2$, and $Z=0.9$. For the SDS case, initially $\rho_{LR} = \sqrt{0.49 \times 0.51} \approx 0.5$, and $Z=0.02$.

B. Measures for the distinguishability

With the respect to the question of whether one can distinguish a pure state from a corresponding mixture with the same populations in the right and left wells. Harris and coworkers [21] showed, in the framework of the wavefunction, that no parity sensitive experiment can measure the difference between them if the states $|L\rangle$ and $|R\rangle$ are taken to be real. They assumed that instantaneous measurements occur on a time scale short compared to that for the system dynamics (tunneling) and compared to that for any interactions with the surrounding molecules. On the contrary, we include an external environment that destroys the right-left coherences in the framework of the density-matrix, and the intermolecular interactions (the homochiral and heterochiral interactions) in the framework of the wavefunction within a mean-field theory.

We investigate the distinguishability between the initially pure and mixed states by measuring a population in the right- well. For the measure, we compare ρ_{RR} of the initially pure vs. mixed state, and for the system with decoherence only, we use $\Delta Z (\equiv Z^P - Z^M)$ where superscripts P and M stand for the initially pure state and the corresponding mixed state.

To examine the distinguishability between the initially pure state and the corresponding mixed state over time, we are required to select the initial conditions for the pure state (X_0^P, Y_0^P, Z_0^P) and the mixed state (X_0^M, Y_0^M, Z_0^M) where $X \equiv 2\text{Re}(\rho_{LR})$, $Y \equiv 2\text{Im}(\rho_{LR})$, and $(X, Y, Z) = (X_0, Y_0, Z_0)$ at $t = 0$. For the maximum contrast between the pure and the mixed state, we choose the same initial population of $|L\rangle$ and $|R\rangle$ in the initial pure and mixed states, i.e. $Z_0^P = Z_0^M$, but choose the degree of initial coherence to be zero for the mixed state (maximum randomness), i.e. $X_0^M = Y_0^M = 0$, while varying initial coherences for the pure state. In other words, when the initially pure state is given by

$$|\Psi(t=0)\rangle = a_{L0}|L\rangle + a_{R0}|R\rangle, \quad (18)$$

or, equivalently,

$$\hat{\rho}^P(t=0) = |a_{L0}|^2|L\rangle\langle L| + |a_{R0}|^2|R\rangle\langle R| + a_{L0}a_{R0}^*|L\rangle\langle R| + a_{R0}a_{L0}^*|R\rangle\langle L|, \quad (19)$$

the corresponding mixed state is given by

$$\hat{\rho}^M(t=0) = |a_{L0}|^2|L\rangle\langle L| + |a_{R0}|^2|R\rangle\langle R|. \quad (20)$$

This initially mixed state may be prepared by making the system interact with an environment that extinguishes the left-right coherence of the system sufficiently fast so that the system dynamics is ignorable.

C. Measures for the degree of decoherence: Purity and off-diagonal elements

In order to measure coherence decay, i.e. , decoherence, we use both the purity and the off-diagonal elements of the reduced density matrix. The purity ς is defined as [22]

$$\varsigma \equiv \text{Tr}(\hat{\rho}^2), \quad (21)$$

where Tr denotes a trace over the system of interest. Note that the decoherence process does not preserve the purity of the state, that is, the purity of the resultant mixed state

becomes less than 1, while that of the pure state is 1. In particular, for a two-level system purity becomes, in the $|L\rangle, |R\rangle$ basis,

$$\text{Tr}(\hat{\rho}^2) = \rho_{LL}^2 + 2|\rho_{LR}|^2 + \rho_{RR}^2, \quad (22)$$

and is given by, in the Bloch-vector representation,

$$\varsigma = \frac{1}{2}(X^2 + Y^2 + Z^2 + 1). \quad (23)$$

As can be easily seen in Eq. (23), $1/2 \leq \varsigma \leq 1$. When the purity decays to a minimum value, $1/2$, this corresponds to $X = Y = Z = 0$, which represents a fully mixed state (a racemic mixture), with equal populations in the right and left wells and with no remaining coherence between them. On the other hand, when the purity remains close to 1, it implies that the system is resistant to the decoherence process. Another more detailed, albeit representation-dependent, measure of decoherence is provided by the decay of off-diagonal reduced density matrix elements. The diagonal elements are the probabilities of finding the system in the corresponding basis state. The off-diagonal elements are a measure of coherence. Specifically, in the $|L\rangle, |R\rangle$ basis, ρ_{LL}, ρ_{RR} are the probabilities of finding the system in the state $|L\rangle$ (left well) and $|R\rangle$ (right well), respectively, and ρ_{LR} is the coherence between the two states. When numerically examining the decoherence rate in terms of the purity decay or the decay of off-diagonal elements, the initially pure states are chosen, rather than the initially mixed states, in order to maximize the influence of initial coherences. That is, $\varsigma(t=0)=1$ ($X_0^2 + Y_0^2 + Z_0^2 = 1$).

D. Computational methods

For the system with decoherence only, we obtained an analytical solution [11]. However, for the system with intermolecular interactions only and the system with both the intermolecular interactions and the decoherence effect, we had to employ computational methods. The terms involved with the stochastic terms η in Eqs.(16) and (17) are integrated by a first order scheme, and the other terms are integrated by the fourth-order Runge-Kutta method. The values of a_L and a_R resulting from the stochastic Schrödinger equation (16) and (17), when averaged over many realizations of the Wiener process, provide the density matrix elements, probabilities and coherences, according to the following relations: $\langle L|\hat{\rho}|L\rangle = \rho_{LL} = \langle a_L a_L^* \rangle$,

$\langle R|\hat{\rho}|R\rangle = \rho_{RR} = \langle a_R a_R^* \rangle$, and $\langle L|\hat{\rho}|R\rangle = \rho_{LR} = \langle a_L a_R^* \rangle$. A time step of 10^{-3} to 10^{-4} and an ensemble of 10^4 realizations were used.

IV. SYSTEM WITH DECOHERENCE ONLY

To provide a simple physical picture focused on the decoherence effect in affecting a tunneling motion between the two wells, we consider a system with decoherence only, i.e., there are no intermolecular interactions and the chiral discrimination energies are zero in Eqs. (16) and (17) ($v = 0$). In our work [11], we study the roles of initial coherences of the system and dephasing rates on the distinguishability of initially pure versus initially mixed states, and the vulnerability to decoherence, i.e., how fast the system will lose its coherence or become a randomly mixed state. In this section we will briefly review the main results of Ref. [11] and then further discuss the effect of the tunneling frequency ω on the distinguishability and the purity decay rate.

A. Review: Effect of initial coherence and dephasing rate

Within a two-level approximation, using $\hat{H} = \hat{H}_0$, for simplicity choosing the energy origin to correspond to $E_m = 0$, i.e., $E_+ = -E_-$, and switching from the density-matrix elements of the states $|L\rangle$ and $|R\rangle$, ρ_{LL} , ρ_{RR} , and ρ_{LR} to the real quantities, X , Y , and Z for the Bloch-vector representation, Eq. (12) gives the following set of equations (see, for details, Ref. [11]) :

$$\frac{dX}{dt} = -4\gamma X, \quad (24)$$

$$\frac{dY}{dt} = -4\gamma Y + 2\omega Z, \quad (25)$$

$$\frac{dZ}{dt} = -2\omega Y. \quad (26)$$

The resultant equations are of standard form [23]. At long times, when the system reaches equilibrium, $dX/dt = dY/dt = dZ/dt = 0$, and the steady-state solution to Eqs. (24)-(26) becomes $X = Y = Z = 0$. This stationary state represents a fully mixed state, with equal populations in the right and left wells and with no remaining coherence between them, and is reached regardless of the initial conditions, the system's tunneling frequency ω , and the dephasing rate γ (related to the nature of the environment and the potential of the system).

With an arbitrary initial state [$X = X_0, Y = Y_0, Z = Z_0$], the general analytical solution (not shown here) can be obtained separately for $\gamma < \omega$ (tunneling dominant region) and for $\gamma > \omega$ (dephasing dominant region). The general solution reveals that, in the dephasing dominant regime for an initially localized state, say $|R\rangle$ (note that this corresponds to an initially chiral state), the system approaches the steady state (fully mixed state) monotonically without any oscillations present but, however, as γ increases, tends to be stuck in the right well on a time scale of $1/\gamma$ (this behavior is equivalent to the quantum Zeno effect [18]). Ref. [11] demonstrated that, as γ increases in this dephasing dominant region, an initially chiral system tends to preserve the chirality, while an initially very delocalized state such as the SDS case tends to become a racemic mixture more quickly. From a general solution to Eqs.(24)-(26), the difference between the time-evolution of Z of the initially pure state and that of the corresponding mixed state, $\Delta Z(\equiv Z^P - Z^M)$ is given by [11]:

$$\Delta Z(t) = -\frac{2\omega Y_0^P}{s} e^{-2\gamma t} \sin(st) \quad \text{for } \omega > \gamma, \quad (27)$$

$$\Delta Z(t) = -\frac{\omega Y_0^P}{\tilde{s}} [e^{(\tilde{s}-2\gamma)t} - e^{-(\tilde{s}+2\gamma)t}] \quad \text{for } \omega < \gamma, \quad (28)$$

with $s = 2\sqrt{\omega^2 - \gamma^2}$ and $\tilde{s} = 2\sqrt{\gamma^2 - \omega^2}$. At a glance, one can easily see that the value of Y_0^P is crucial to the distinguishability. If $Y_0^P = 0$, $\Delta Z(t) = 0$, which means no distinguishability, for all time and for all γ . However, if $Y_0^P \neq 0$ the distinguishability does exist, although it disappears over time because the decoherence impels both the initially pure state and the corresponding mixture to the maximally randomized stationary state. For the tunneling dominant region, as γ increases, the period of the oscillation increases and the amplitude decays faster, leading to ΔZ approaching zero more rapidly, at which point one can not tell whether the system was initially in the pure state or in the corresponding mixture upon the measurement of population. However, for the dephasing dominant region, as γ increases, the distinguishability disappears more slowly, suggesting that considerably strong dephasing may unexpectedly afford means to observe the long-time surviving distinguishability. Noting that for a two-level system purity is given by Eq.(23) and using Eqs.(24)-(26), one can obtain

$$\frac{d\zeta}{dt} = -4\gamma(X^2 + Y^2). \quad (29)$$

In our previous work [11], the interplay of the initial coherence and the dephasing rate on the purity decay, in particular, as it relates to the racemization and chirality stabilization, was clarified. For very short times, increasing the dephasing rate γ and the initial coherences

$(X_0^2 + Y_0^2 = 4|\rho_{LR}|^2)$ increases the purity decay (decoherence) rate. On the other hand, for later times, for larger initial coherences ($X_0^2 + Y_0^2 \approx 1$), the purity still tends to decay faster with increasing γ , but for the smaller initial coherences ($X_0^2 + Y_0^2 \approx 0$), the purity shows the opposite behavior when γ is increased beyond a certain threshold, i.e., the purity decay starts to be suppressed. This interesting observation enables us to suggest that, in the environment destroying the left-right coherences, on a timescale faster than the intra-system dynamics (the tunneling time scale), the initially strongly localized state would tend to preserve the chirality, while, on the other hand, an initially strongly delocalized state such as a superposition of the two chiral states, would become a racemic mixture very quickly. It is notable that the observation agrees with the prediction that if the system dynamics is ignorable compared with the interaction between the system and the environment, the coherence between the eigenstates of the decohering operator will be lost fastest [12, 16]. The applicability of the prediction can be seen by realizing that the two chiral states $|L\rangle$ and $|R\rangle$ correspond to the eigenstates of the decohering operator ($\hat{\sigma}_z = |R\rangle\langle R| - |L\rangle\langle L|$), and the stronger dephasing rate beyond a certain threshold allows us to ignore the system dynamics compared with the decoherence process. Then, according to the prediction, a superposition of the two chiral states will lose its coherence much faster than a localized chiral state ($|L\rangle$ or $|R\rangle$). However, it is also notable that there was previously no prediction for the observation in Ref. [11] that increasing the initial coherences ($X_0^2 + Y_0^2$) leads to a system that exhibits more rapid decoherence.

B. Tunneling frequency ω ($=\delta/\hbar$)

The typical behavior of $\Delta Z(t)$ for several values of ω for a given value of γ (here chosen as 1) is shown in Fig. 1 (a) and (b). For $\omega < \gamma$ (dephasing dominant region, here $\omega < 1$, shown in (a)), as time increases $\Delta Z/Y_0^P$ first decreases from zero to a minimum and then increases monotonically towards zero. Note that, as ω increases, the maximum of $|\Delta Z/Y_0^P|$ gets larger and is obtained at an earlier time, i.e., t_{\max} gets smaller and the distinguishability disappears more rapidly beyond t_{\max} (i.e. $\Delta Z/Y_0^P$ goes to zero more quickly). For instance, compare the cases $\omega = 0.1$ and $\omega = 0.8$ in Fig. 1 (a). For the case $\omega = 0.1$, $|\Delta Z/Y_0^P| = 0.0494$ at $t = t_{\max} \approx 1.5$, and, is still nonzero at $t = 8$ having a value of 0.0464 which is roughly the same as the maximum value of $|\Delta Z/Y_0^P|$, indicating

the long-time surviving distinguishability, while for the case $\omega = 0.8$, $|\Delta Z/Y_0^P| = 0.315$ at $t = t_{\max} = 0.58$, and is almost zero at $t = 8$, indicating no distinguishability for $t > 8$. This observation suggests that a very slow tunneling oscillation may unexpectedly allow us to observe the long-time surviving distinguishability. On the other hand, for $\omega > \gamma$ (tunneling dominant region, here $\omega > 1$, shown in (b)), as ω increases, the period of the oscillation in ΔZ decreases, but the amplitude envelope decays exponentially with a rate that is almost independent of ω . In other words, for the tunneling dominant region, the rate with which ΔZ approaches toward zero is largely determined by γ , as expected from Eq.(27). For all the cases $\omega = 2, 4, 6$ [Fig. 1 (b)], upon the measurement of population after $t = 3$, one can not tell whether the system was initially in the pure state or in the corresponding mixture. Figure 1(c) captures well the effect of increasing the tunneling frequency of the system on the purity decay at a given $\gamma (= 1)$. Initially the system was prepared in the $|R\rangle$ state (the LS case). Interestingly and non-intuitively, increasing the tunneling frequency ω tends to increase the rate of purity decay rather than reducing it. For the case $\omega=0.2, 0.4$ and 0.8 (the dephasing dominant region), increasing ω clearly accelerates the purity decay for all time. Even for the case $\omega = 2, 4$, and 8 (the tunneling dominant region) where the oscillatory decay becomes visible, the purity decay rate increases with increasing ω at short times, while the overall decay timescale appears to be dominated by the dephasing rate γ . In regard to the quantum-classical transition, realizing that a smaller ω corresponds to a higher inter-well barrier, a longer tunneling time, and thus a more classical system, the observation that decreasing ω decreases the decoherence rate can be put in the following way; a more classical (quantum) system is less (more) vulnerable to decoherence. It is also noteworthy that the master equation of the system of interest in this section (the chiral system within a two-level approximation in the presence of an environment destroying the coherence between the two states, see Eqs. (24) to (26)) is identical to that resulting from a two-level atom driven by a field undergoing a pure dephasing [24] in quantum optics, as previously mentioned in Ref. [18]. This equivalency emerges where the following replacements are made: $|L, R\rangle \rightarrow$ the two energy eigenstates, $\omega \rightarrow$ Rabi-frequency, and $\gamma \rightarrow$ pure dephasing rate. Noting this equivalency enables us to recognize that the above observation (increasing ω tends to increase the purity decay rate) is also equivalent to the result of Ref. [25], where aspects of coherence and decoherence were studied with a two-level system interacting with a decohering environment and a resonant continuous-wave

electromagnetic field, that increasing the Rabi frequency increases the decoherence rate.

V. SYSTEM WITH INTERMOLECULAR INTERACTIONS ONLY

The system with intermolecular interactions within a mean-field approximation was studied in Ref. [5], with a particular focus on the role of intermolecular interactions in establishing chiral stability. Localized chiral states were shown to be stable when the homochiral interactions are energetically favorable to heterochiral interactions ($v > 0$), whereas delocalized states are dominant when the heterochiral interactions are energetically favorable ($v < 0$). For a self-completeness and a later comparison with the case in the presence of both the intermolecular interactions and the decoherence effect, we reproduce some of the results of Ref. [5], with emphasis on the interplay of the chiral discrimination energy parameter v and the initial condition of the system in establishing the anharmonic oscillations in population of the two wells of the system. In subsection VB we show that a nonzero chiral discrimination energy can bring about the distinguishability between the initially pure and the corresponding mixed states even for the $Y_0^P = 0$ case, where there is no distinguishability in the system in the absence of the intermolecular interactions ($v = 0$), regardless of the decoherence effect, as shown subsection IV.

A. Review

The system with intermolecular interactions only is described by Eqs.(16) and (17) with $\Gamma = 0$. Below for all the numerical calculations Ω is chosen as 1. The time-evolution of the initially localized state $|R\rangle$ (the LS case) with a variation of v is shown in Fig.2. For the $v = 0$ case we see coherent tunneling from one well to the other. As $|v|$ increases (the chiral energy difference $|V_{het} - V_{hom}|$ increases), the nonlinearity of the differential equations increases and the oscillations in population between the two wells becomes anharmonic. For a sufficiently large $|v|(> 4)$ and with increasing $|v|$, population-trapping becomes stronger and maximum coherence decreases. We observed a similar relation between the coherence $|\rho_{LR}|^2$ and the self-trapping in the WDS and the SDS cases (not shown here): when self-trapping due to intermolecular interactions is manifested in ρ_{RR} , $|\rho_{LR}|^2$ is seen to exhibit a decrease in the oscillation amplitude, and thus a decrease in the maximum coherence, which prohibits

a complete tunneling between the two wells, and consequently results in the self-trapping of population. Considering that characteristic values of the chiral discrimination energy difference, $|V_{het} - V_{hom}|$, are far greater than the tunneling splitting δ , i.e. , $|v| \gg 1$ [26], Fig. 2(a) demonstrates that much of the system in a condensed phase can be self-trapped in one of the enantiometric forms to a degree which depends on the chiral discrimination energies (i.e. V_{het} and V_{hom}). As demonstrated in Fig. 2, behaviors of ρ_{RR} , $|\rho_{LR}|^2$, and thus the self-trapping effect are independent of the sign of $|v|$ for the initially localized state (LS case). Note that the LS case has no initial coherence between $|L\rangle$ and $|R\rangle$, i.e. , $\rho_{LR}(t = 0) = 0$. However, when there exist nonzero initial coherences, the stability of the initial states does depend on the sign of $|v|$, i.e. , whether the homochiral mixture is energetically favorable ($v > 0$) or the heterochiral mixture is favorable ($v < 0$). We present two cases of different initial coherences, the WDS and SDS cases, for several values of v . For the WDS case with positive v [Fig. 3(a)], as v increases from 0 to 2 the oscillation period of ρ_{RR} increases and then decreases beyond $v = 2$ with the population becoming self-trapped for $v \geq 5$. This observation is similar to that of the LS case. However, when v is negative [Fig. 3(b)], this initially small degree of delocalization leads the system to oscillate between the two wells (chiral activity) with a faster oscillation frequency than that of the $v = 0$ case, until v reaches quite a large magnitude, for instance, $v = -10$, when the system is now self-trapped again. Comparisons of the $v = 5$ and the $v = -5$ cases show how the initially weakly delocalized state (the WDS case) can behave very differently depending on the sign of v . For large negative v (e.g., $v = -10$) the system becomes self-trapped. For large positive v (e.g., $v = +5$) the system also becomes self-trapped, but such a trapping is stable in sense that it remains self-trapped as v is further increased. For positive v in the WDS case the self-trapping becomes very stable, while for the negative v the tunneling is more assisted and stabilized by the addition of the intermolecular interactions. This behavior is shown in the exactly opposite way for the SDS case, since the initial conditions with almost equal populations in each well ($a_L \approx a_R$) correspond to stable states for negative v but unstable states for positive v . With positive v [Fig. 4(a)] the initially strongly delocalized state exhibits oscillations about $\rho_{RR} \approx 0.75$ for $v = 5$ and $\rho_{RR} \approx 0.7$ for $v = 10$, indicating that the system is chiral active, whereas as for $v = 0$ and $v = 2$, ρ_{RR} exhibits a small amplitude oscillations about ~ 0.5 , indicating that the system is not chiral active. On the other hand, for negative v [Fig. 4(b)] the delocalized state becomes very stable around $\rho_{RR} = 0.5$ with

an oscillation frequency that increases with increasing $|v|$.

B. Distinguishability of pure and mixed states

One of the main motivations of this paper was to answer some questions arising from Vardi’s claim in the last paragraph of Ref. [5]. He argued that from the results “... *In the former case, spontaneous symmetry breaking may take place, turning a nearly racemic mixture into an optically active ensemble.*” Since his model does not associate with any decoherence source, the system remains pure if it is initially pure. All of his results were obtained for initially pure states. Thus when he used “racemic mixture”, it would have been correctly described as a delocalized pure state as opposed to a racemic mixture that is found in nature and associated with loss of coherences. At this point we face two questions. First, if the system starts as a mixed state, then will it show results similar to those of initially pure states? This question may be put as follows: can we distinguish the initially pure and the initially mixed states for the system with intermolecular interactions? If we cannot do so by measuring populations, for instance, ρ_{RR} , then Vardi’s claim may be justifiable. Otherwise, decoherence should be seriously considered to answer the second question: how can an initially pure state end up as a nearly racemic mixture or an optically active ensemble in real system? We attempt to answer the first question here and the second one in the next section. We start by showing the time-evolutions of population and coherence in Fig. 5 with the initially pure and the corresponding mixed state for the WDS and SDS cases (note that for both of these cases $Y_0^P = 0$) in the absence of the intermolecular interactions ($v = 0$). Figure 5(a) demonstrates that when $Y_0^P = 0$, there is no distinguishability in terms of the population ($\Delta Z = 0$), as already seen in Eqs. (27) and (28), whereas there are clear differences in terms of the coherence as shown in Fig. 5(b). Now we proceed the issue of distinguishability of the initially pure and mixed states for the system with the intermolecular interactions. In the previous section V A, changing the initial condition from the LS case to the WDS and SDS cases, and thus creating nonzero initial coherence is seen to lead the system to behave differently depending on the sign of v . Thus, one may imagine that the initially mixed state without initial coherences may behave differently from the initially pure state with nonzero initial coherence, even when $Y_0^P = 0$ such as in the WDS and the SDS cases. We compare the initially pure state for the WDS and SDS with their corresponding

mixed states, in terms of the population and the coherence, in particular, for $v = 5$ and $v = -5$. Figure 5(c) demonstrates that for the WDS case a nonzero v enables one to tell whether the system was initially in a pure or a mixed state by measuring populations. The pure state is observed to behave differently, depending on the sign of v , while the behavior of the corresponding mixed state is independent of the sign of v due to the absence of its initial coherence. Since the WDS case is slightly delocalized from the LS case, the behavior of the population (as measured by ρ_{RR}) of the initially mixed state for the WDS case is quite close to that of the pure state of the LS case [Fig. 5(c)]. For the SDS case, the similar distinguishability, brought about by the nonzero v , is seen in Fig. 5(d). Let us clarify the behavior of the initially mixed state related to the LS case with the same $v(= \pm 5)$: one can note that ρ_{RR} of the mixed state for the WDS and SDS cases is seen to oscillate in the same way as that of the initially pure state for the LS case with the same v and differences are found only in the amplitude and the associated mean value ρ_{RR} (as obtained by averaging over an oscillation cycle) [Figs. 5(c) and 5(d)]. When the initially pure state is given by Eq. (18), the corresponding mixed state is chosen by Eq. (20). Then, the probability of being in the right well for the initially mixed state, $\rho_{RR}^M(t) = \langle R | \hat{\rho}^M(t) | R \rangle$ can be expressed in terms of the probability of being in the right well for the LS case (denoted as $|a_R^{RR}(t)|^2$):

$$\rho_{RR}^M(t) = \langle |a_R|^2 \rangle, \quad (30)$$

$$= |a_{L0}|^2 |a_R^{LL}(t)|^2 + |a_{R0}|^2 |a_R^{RR}(t)|^2, \quad (31)$$

$$= |a_{L0}|^2 + (|a_{R0}|^2 - |a_{L0}|^2) |a_R^{RR}(t)|^2. \quad (32)$$

where $|a_R^{LL}(t)|^2$ ($|a_R^{RR}(t)|^2$) denotes the probability of being in the right well at time t for the state initially localized in $|L\rangle$ ($|R\rangle$). Here we used $|a_R^{LL}(t)|^2 = 1 - |a_L^{LL}(t)|^2 = 1 - |a_R^{RR}(t)|^2$: the second equality holds since Eqs. (16) and (17) with $\Gamma = 0$ (decoherence-free case) are L-R symmetric. The above Eq. (32) indicates that the probability of the initially mixed state should have the same oscillation period as that of the initially pure state localized in $|R\rangle$ (LS case) with the same v , but the amplitude and average of the probability of the former are changed from those of the latter, depending on its $|a_{L0}|^2$, and $|a_{R0}|^2$. For the SDS case, for instance, since $|a_{L0}|^2 = 0.49$, and $|a_{R0}|^2 = 0.51$, ρ_{RR}^M of the initially mixed state with $v = \pm 5$ oscillates from 0.51 to 0.506 in tune with ρ_{RR}^P of the initially pure state localized in $|R\rangle$ (LS case) ($= |a_R^{RR}(t)|^2$) with the same $v(= \pm 5)$ which oscillates from 1 to 0.8 [Fig. 5(d)]. The similar observation is made in the WDS case as well [Fig. 5(c)]. As clearly demonstrated

in Figs. 5(c) and 5(d), for a system with intermolecular interactions, the initially mixed state behaves differently from the initially pure state as measured by the probabilities. In addition, the initially mixed state does not behave differently depending on the sign of v . Thus, Vardi's claim is unjustifiable. For instance, an initially nearly racemic mixture remains as a racemic mixture, regardless of whether the chiral discrimination energy favors the homochiral mixture or the heterochiral mixture, as shown in Fig. 5(d). Now it seems very critical to include the initial coherences adequately to obtain the correct behavior of the system subject to the intermolecular interactions. Further, if one were to create a nearly racemic mixture or an optically active ensemble in laboratory, starting from an initially pure state, it would be essential to include the decoherence process in the assessment and modeling of the system dynamics. We explore this in the following section.

VI. SYSTEM IN THE PRESENCE OF BOTH DECOHERENCE AND INTERMOLECULAR INTERACTIONS

In this section, we finally consider the system in the presence of both a decoherence effect and intermolecular interactions. In Section IV we discussed general features of the decoherence effect on the system without chiral discrimination energies, i.e., $v=0$. Two prominent system behaviours were observed: suppressing the tunnelings (oscillations) between the two chiral states by destroying the coherence, and forcing the system to the long-time mixed state with a complete randomness, $\hat{\rho}(t \rightarrow \infty) = \frac{1}{2}(|L\rangle\langle L| + |R\rangle\langle R|)$, regardless of the dephasing rate and the initial condition as long as the decoherence is present. In the study of the decoherence effect on a system having the intermolecular interactions, the former is observed, while the latter does not occur for all cases. The long-time stationary state is observed to be dependent on the decoherence strength Γ , the initial condition of the system, and the chiral discrimination energy parameter v . Details are as follows. In particular, we examine three different classes of initial conditions: the LS, WDS, and SDS cases. We apply Eqs.(16) and (17). Coherence losses are monitored by measuring the purity rather than $|\rho_{LR}|^2$ since the purity enables us to compare easily the cases with different maximum coherences and is representation-independent. We point out that all decoherence-free cases were presented up to $t = 5$ (Figs. 2 to 4), while the cases with the decoherence will be presented up to $t = 20$ to reveal the longer-time behavior. We varied Γ from 1.6×10^{-4} to 1.6×10^{-2} , which

means that dephasing time is very long compared with tunneling time (tunneling dominant region). Figures 6(a) and 6(b) show behaviors of the population and the purity for several values of v at a very small decoherence (here chosen as $\Gamma = 1.6 \times 10^{-4}$) for the LS case. None of the cases examined here reached a stationary state within $t = 20$. As expected, introducing decoherence results in decay of the oscillation amplitudes of both the population and the purity. Details are affected by $|v|$: for such a small decoherence ($\Gamma = 1.6 \times 10^{-4}$), the $v = 0$ case is seen to make no significant changes within a time window of $t = 20$, while cases with a nonzero v tend to experience relatively significant changes, suggesting that the intermolecular interactions make the system more vulnerable to decoherence. However, the decoherence rate is not exactly proportional to $|v|$. A relative sensitivity to decoherence depending on the magnitude of v is more clearly seen from comparing the purity decay for several cases with different v in Fig. 6(b). The order in the rate of purity decay R is $R(v = \pm 4) > R(v = \pm 3.9) > R(v = \pm 3) > R(v = \pm 5) > R(v = \pm 10)$. From the behavior of ρ_{RR} for the decoherence-free case shown in Fig. 2(a), one can see that until $|v|$ becomes large enough to cause the self-trapping ($v = \pm 5, \pm 10$), the purity decay rate R increases with increasing $|v|$. However, when the self-trapping occurs, R becomes smaller than other cases that show no self-trapping, and tends to be smaller with a stronger self-trapping, i.e., greater v . This trend is also observed in the LS case with larger Γ , $\Gamma = 1.6 \times 10^{-3}$ in Fig. 6(c) and $\Gamma = 1.6 \times 10^{-2}$ in Fig. 7(a). For instance, consider the case with $v = \pm 10$, which induces a very strong self-trapping [Fig. 2(a)]. The purity decay rate for $v = \pm 10$ is almost overlapped with that for $v = 0$ with $\Gamma = 1.6 \times 10^{-4}$ [Fig. 6(b)] and $\Gamma = 1.6 \times 10^{-3}$ [Fig. 6(c)], and even becomes smaller than that for $v = 0$ with $\Gamma = 1.6 \times 10^{-2}$ [Fig. 7(a)]. It suggests that for some chiral discrimination energies, especially those inducing a strong self-trapping (localization), the resistance to decoherence can be stronger than for the $v = 0$ case, whereas, for values of v not inducing strong self-trapping the opposite effect is seen with respect to decoherence, namely the non-zero v case is more sensitive to decoherence than the $v = 0$ case. It is noteworthy that the effect of chiral interactions on the LS case is very similar to that of decoherence; for the initially localized state, namely purity decay is accelerated with increasing decoherence, but starts to be suppressed with continued increase in decoherence beyond a certain threshold decoherence [11]. Figures 7(a) and 7(b) show that for $\Gamma = 1.6 \times 10^{-2}$ both of the purity ($t \rightarrow \infty$) and $\rho_{RR}(t \rightarrow \infty)$ for the LS case tend to be larger for a larger $|v|$, implying that for a bigger chiral discrimination energy the system

relaxes to a stationary state with greater chirality. Specifically, within $t = 20$, for $v = \pm 3$, the system will be relaxed to a racemic mixture ($\rho_{RR} \rightarrow 0.5$), whereas, for $v = \pm 10$, the system will preserve its chirality as $\rho_{RR} > 0.95$ at $t = 20$ [Fig. 7(b)]. Also it is notable that the purity for $v = \pm 3$ has a stationary value of roughly 0.57, whereas the purity for $v = \pm 10$ does not decay much from the initial value ($=1$), being 0.96 at $t = 20$ [Fig. 7(a)]. This can be understood by realizing that, from comparison with the decoherence-free cases shown in Fig. 2(a), $v = \pm 10$ stabilizes the initially localized state by self-trapping it to the initially located well, and this effect will not be much affected by the decoherence inhibiting the oscillations between the two wells. On the other hand $v = \pm 3$ does not bring about that kind of self-trapping effect, and rather makes the system anharmonically oscillate between the two wells, which would be prohibited by the loss of coherences in the presence of decoherence. For the LS case, the stronger the self-trapping, the less vulnerability to decoherence. Also, in relation to stationary values of the purity and ρ_{RR} , for $v = \pm 3$, the observation that the purity $\rightarrow 0.57$ and $\rho_{RR} \rightarrow 0.5$, implies that, from Eq. (22), ρ_{LR} does not relax to zero ($|\rho_{LR}|^2$ goes to roughly 0.04), and the system can have therefore gained coherence due to the combined influence of the decoherence, the intermolecular interactions, and the initial condition. It is also notable that decoherence brings the purity and population (ρ_{RR}) for $v = \pm 3.9$ and ± 4 cases quite close together, as shown in Fig. 7(a) and [Fig. 2(b)], respectively, smoothing out the dramatic differences between them in the absence of decoherence [Fig. 2(a)]. To see the effect of increasing decoherence on the population relaxation and the purity decay for a given v , we present ρ_{RR} and the purity for $v = 5$, with several values of Γ , in Fig. 8. As decoherence Γ increases, the rate of relaxations in both the population and the purity increases. Also it is notable that both of $\rho_{RR}(t \rightarrow \infty)$ and the purity ($t \rightarrow \infty$) tend to decrease with increasing Γ , implying that with increasing Γ the $v = 5$ case tends to approach a less chiral stationary state. Therefore, by inducing the loss of coherences between the two states and thus leading to the suppression of the oscillation (tunneling), decoherence can bring to a system a stabilization of the chirality with $\Gamma = 1.6 \times 10^{-3}$, or a less chiral state (or possibly racemization) with $\Gamma = 1.6 \times 10^{-2}$, as determined by the interplay of the decoherence (Γ) and the intermolecular interactions (v). Now let us turn to the opposite case, the initially strongly delocalized state (SDS) case. The results of the SDS case are presented in Fig. 9 with a variation of v at $\Gamma = 1.6 \times 10^{-3}$. First, in regard to the relative order of the purity decay, one can easily see that the stronger the chiral discrimination en-

ergy (v), the faster the purity decays, i.e. , the larger the decoherence rate is [Fig. 9]: with positive v , $R(v = 2) < R(v = 3) < R(v = 5) < R(v = 10)$ [Fig. 9(b)], and with negative v , $R(v = -2) < R(v = -3) < R(v = -5) < R(v = -10)$ [Fig. 9(d)]. Unlike the LS case, an exception is not found in the SDS case due to non-existence of self-trapping state in the SDS case for parameter ranges considered here [Fig. 4]. Second, the SDS case with positive v is seen to be more vulnerable to decoherence than that with negative v . For the SDS case, as shown in Fig. 4, time-evolution of population of the initially strongly delocalized state ($a_L \approx a_R$) depends strongly on the sign of v . When there is no decoherence effect, for negative v , the ρ_{RR} oscillates in a narrow range about $\rho_{RR} \approx 0.5$ whereas for positive v , ρ_{RR} oscillates over a much wider range between $\rho_{RR} \approx 0.5$ and $\rho_{RR} \approx 1$. That is, the initially strongly delocalized state becomes stable for negative v but unstable for positive v . This feature continues to be effective upon introducing the decoherence effect, and thus the SDS case shows a faster purity decay and a faster population relaxation for positive v than for negative v [Fig. 9]. It suggests that a critical difference in the stability of the initial states, depending on the sign of v , i.e. , whether the heterochiral interactions are stronger or weaker than the homochiral interactions, affects the sensitivity of the system to the decoherence effects. This is reconfirmed in the WDS case ($a_L \ll a_R$) for which results are presented in Fig. 10 with a variation of v at $\Gamma = 1.6 \times 10^{-3}$. In contrast to the SDS case [Fig. 9], the WDS case with negative v is more vulnerable to decoherence than that with positive v . For the WDS case in the absence of decoherence, when the homochiral mixture is preferred (the positive v), the initially weakly delocalized state becomes stabilized, while, when the heterochiral mixture is preferred (negative v), the initial state becomes highly unstable and the system leads to the facilitated tunneling [Fig. 3]. Thus, upon introducing the decoherence, the system with positive v shows a less vulnerability to the decoherence, i.e. , a slower purity decay and a slower population relaxation, than the corresponding cases with negative v [Fig. 10]. It is very interesting to see that the character of intermolecular interactions can change the sensitivity of the system to the decoherence, by (de)stabilizing the initial state. On the other hand, for the WDS case, the relative sensitivity to the decoherence seems to have a rather complicated dependence on v due to its medium sized initial coherence, compared with the two extreme cases, the LS and SDS cases. The effects of increasing decoherence on the WDS and SDS cases for a given v are demonstrated in Figs. 11 and 12, respectively. Similarly to the LS case, for a given v , in both of the WDS and SDS cases, one can see

that the larger the decoherence is, the faster the purity decays and the faster the population relaxes. Further, related to the homochiral/heterochiral preferences in the intermolecular interactions, introducing decoherence does not necessarily lead to the breakdown of the homochiral/heterochiral preference. For the WDS case, for instance, a value of $v = 5$ yields a system with a homochiral preference when $\Gamma = 1.6 \times 10^{-3}$ ($\rho_{RR}(t \rightarrow \infty)$ is expected to be greater than 0.9 as shown in Fig. 11(a)), while a value of $v = -5$ results in a racemic mixture without chirality, reflecting its heterochiral preference for the same value of Γ [Fig. 11(c)]. Similarly, for the SDS case, at all Γ examined here, for $v = 5$ $\rho_{RR} \rightarrow 0.51$ [Fig. 12(a)], implying a small homochiral preference. For $v = -5$ ρ_{RR} is expected to relax to 0.5 with oscillations around 0.5, implying the heterochiral preferences [Fig. 12(c)].

VII. CONCLUSION

We studied the effects of chiral intermolecular interactions and decoherence on the distinguishability between the initially pure and mixed states, and the chirality stabilization in a chiral system. A two-level approximation was adopted for the system. Chiral intermolecular interactions were introduced within a mean-field theory. The interaction of the system with an environment (to take account for externally induced decoherence) was modeled as a continuous position measurement of the system, which reduces to a measurement of a population difference between the two chiral states. To better understand the combined effects of the two interactions, we first investigated the system in the presence of each interaction separately. For the system with decoherence only, most features is studied in Ref.[11] where we obtained the following results (which we presented in summarized form in this work). When Y_0^P is nonzero, for the dephasing dominant region, increasing the tunneling frequency can lead to long-time survival of distinguishability, while for the tunneling dominant region, the timescale of the distinguishability is largely dominated by the dephasing rate. For the initially $|R\rangle$ state (LS), decreasing the tunneling frequency tends to suppress the purity decay, suggesting that the more classical system is less vulnerable to decoherence. In the system with chiral intermolecular interactions only, we showed that the nonzero chiral discrimination energies can bring about the distinguishability between the initially pure and the corresponding mixed states even when $Y_0^P = 0$, where no distinguishability exists in the absence of the intermolecular interactions. Finally, we introduced both decoherence

and intermolecular interactions to the system, and then explored the combined effects on the purity decay rate and the stationary states of the system with several different initial conditions. The dephasing time was varied to be relatively very long compared with tunneling time (tunneling dominant region) so that the decoherence process in the absence of chiral intermolecular interactions is very slow. However, when combined with the chiral intermolecular interactions, the decoherence process tends to be accelerated. For a given chiral discrimination energy v , we showed that, similar to the case with decoherence only, the purity decays faster as the dephasing rate increases. For a given dephasing rate, the purity decay was shown to be influenced by v and the initial state of the system. As the chiral discrimination energy $|v|$ increases, the SDS case is observed to have a faster purity decay, while the LS case to have a purity decay suppressed beyond a certain threshold $|v|$ because of onset of induced self-trapping. This is very similar to the interplay of the initial coherence of the system and the dephasing rate on the purity decay in the system with decoherence only. Also we clarified the role of the sign of v associated with the initial state on the purity decay. For the WDS case, the purity is seen to decay slower with positive v than with negative v since positive v , which prefers homochiral mixtures, stabilizes the initially weakly delocalized state. For the SDS case, the opposite is true. The results should serve as a prototype for understanding the results of a chiral system in more complicated and realistic conditions, such as systems with more than two degrees of freedom (beyond a two-level approximation) and with other types of environment, for instance, which induces both population loss (energy relaxation) and phase loss (dephasing). This work may be extended to an open chiral system interacting with lasers. In recent years, there has been increasing interest on the control of molecular chirality [9, 10]. However, the decoherence effect and the intermolecular interactions on these preparation/control scenarios are far from well understood. Realizing that the decoherence process can be detrimental to the control scenarios by destroying the very coherence that is needed for the control scenario, it would be critical to understand and include the decoherence process properly when the time scales of system dynamics, and/or environmental effects (energy loss, dephasing) are comparable to the interaction time scale between the system and the laser field. In addition, our results suggest that taking into account these effects may be important even when the decoherence time scale is not comparable to or longer than other time scales, since a system with nonzero chiral discrimination energies tends to be more vulnerable to decoherence, i.e. , tends to have

a faster purity decay than a system without chiral intermolecular interactions.

Acknowledgements

It is a pleasure to acknowledge the Natural Sciences and Engineering Research Council of Canada for financial support in the form of a Discovery Grant.

-
- [1] F. Hund, Z. Phys. **43**, 805 (1927).
- [2] J. J. Sakurai, *Modern Quantum Mechanics* (Addison-Wesley Publishing Company, Inc., 1985), Chap 4.
- [3] S. F. Mason, *Molecular Optical Activity and the Chiral Discriminations* (Cambridge University Press, Cambridge, 1982), Chap 11; G. E. Tranter, Nature (London) **318**, 172 (1985).
- [4] E. B. Davies, Commun. Math. Phys. **64**, 191 (1979); A. Koschany, J. Kuffer, G. M. Obermair, and K. Plessner, Phys. Lett. A **185**, 412 (1994).
- [5] A. Vardi, J. Chem. Phys. **112**, 8743 (2000) .
- [6] R. Silbey and R. A. Harris, J. Phys. Chem. **93**, 7062 (1989).
- [7] P. Pfeifer, Phys. Rev. A. **26**,701 (1982).
- [8] B. Fain, Phys. Lett. A **89**, 455 (1982).
- [9] J. A. Cina and R. A. Harris, J. Chem. Phys. **100**, 2531 (1994); R. P. Duarte-Zamorano and V. V. Romero-Rochin, J. Chem. Phys. **114**, 9276 (2001).
- [10] M. Shapiro, E. Frishman, and P. Brumer, Phys. Rev. Lett. **84**, 1669 (2000); Y. Fujimura, L. Gonalez, K. Hoki, J. Manz, and Y. Ohtsuki, Chem. Phys. Lett. **306**, 1 (1999).
- [11] H. Han and D. M. Wardlaw, Chem. Phys. Lett. (2008), submitted.
- [12] I. O. Stamatescu, E. Joos, H. D. Zeh, C. Kiefer, D. Giulini, and J. Kupsch, *Decoherence and the Appearance of a Classical World in Quantum Theory*, 2nd ed. (Springer Verlag, 2003).
- [13] H. Han and P. Brumer, J. Chem. Phys. **122**, 144316 (2005) and references are therein.
- [14] E. Joos and H.D. Zeh, Z. Phys. B **59**, 223 (1985).
- [15] A.O. Caldeira and A.J. Leggett, Physica A **121**, 587 (1983).
- [16] W. H. Zurek, Rev. Mod. Phys. **75**, 715 (2003); P. Blanchard, D. Giulini, E. Joos, C. Kiefer, I. O. Stamatescu (eds), *Decoherence: Theoretical, Experimental, and Conceptual Problems*, 2nd ed. (Lecture Notes in Physics 538, Springer Verlag, 2000).
- [17] M. R. Gallis and G. N. Fleming, Phys. Rev. A **42**, 38 (1990).
- [18] M. J. Gagen, H. M. Wiseman, and G. J. Milburn, Phys. Rev. A **48**, 132 (1993); G. J. Milburn, J. Opt. Soc. Am. B **5**, 1317 (1988).
- [19] N. Gisin and I. Percival, J. Phys. A **25**, 5677 (1992) and references are therein.
- [20] A. Smerzi, S. Fantoni, S. Giovanazzi, and S. R. Shenoy, Phys. Rev. Lett. **79**, 4950 (1997).

- [21] R. A. Harris, Y. Shi, and J. A. Cina, *J. Chem. Phys.* **101**, 3459 (1994).
- [22] P.C. Lichtner and J.J. Griffin, *Phys. Rev. Lett.* **37**, 1521 (1976); W.H. Zurek, S. Habib and J.P. Paz, *Phys. Rev. Lett.* **70**, 1187 (1993); M. C. Nemes and A.F.R. deToledo Piza, *Physica (Amsterdam)* **137A**, 367 (1986); X-P. Jiang and P. Brumer, *Chem. Phys. Lett.* **208**, 179 (1993).
- [23] H. C. Torrey, *Phys. Rev.* **76**, 1059 (1949).
- [24] D. F. Walls and G. J. Milburn, *Quantum Optics* (Springer Verlag, 1994); M. O. Scully and M. S. Zubairy, *Quantum optics* (Cambridge University Press, 1997).
- [25] A. S. Sanz, H. Han, and P. Brumer, *J. Chem. Phys.* **124**, 214106 (2006).
- [26] I. Alkorta, O. Picazo, and J. Elguero, *Curr. Org. Chem.* **10**, 695 (2006); J. Ka and S. Shin, *J. Mol. Struct.* **623**, 23 (2003).

FIGURE CAPTIONS

Fig. 1. Dependence of distinguishability and decoherence process on tunneling frequency ω as a function of time for the decoherence only case. Distinguishability versus time as measured by $\Delta Z(t) (\equiv Z^P(t) - Z^M(t))/Y_0^P$ is depicted for the dephasing dominant region $\omega < 1$ in panel (a) and for tunneling dominant region $\omega > 1$ in panel (b). The values of ω are indicated in the legend and included in both panels to provide a comparison. Purity vs. time is depicted in panel (c) for a range of ω values; γ is chosen as 1. All the variables are in dimensionless units.

Fig. 2. Time evolution of population ρ_{RR} and coherence $|\rho_{LR}|^2$ are shown for the LS case with $v = 0$ (thick line), ± 3 (\cdots), ± 3.9 ($-\cdot-\cdot-$), ± 4 ($---$), ± 5 ($-.-.-$), and ± 10 (thin line).

Fig. 3. Time evolution of ρ_{RR} is shown for the WDS case with various values of v . (a): $v = 0$ (thick line), 2 ($---$), 3 (\cdots), 5 ($-.-.-$), and 10 (thin line). (b): $v = 0$ (thick line), -2 ($---$), -3 (\cdots), -5 ($-.-.-$), and -10 (thin line).

Fig. 4. Time evolution of ρ_{RR} is shown for the SDS case with various values of v . (a): $v = 0$ (thick line), 2 ($---$), 3 (\cdots), 5 ($-.-.-$), and 10 (thin line). (b): $v = 0$ (thick line), -10 (thin line). Note the difference in the scale of ordinate in panels (a) and (b).

Fig. 5. Time evolution of ρ_{RR} and $|\rho_{LR}|^2$ are shown with various initial conditions. For (a) and (b), $v = 0$ and four different initial conditions are presented: the initially pure state for the WDS case ($---$), the initially pure state (\cdots) for the SDS case, and the corresponding mixed states are presented as (squares) and (circles), respectively. For comparison, the LS case with $v = 0$ is also presented ($---$). Panels (c) and (d) display the WDS and SDS cases, respectively, with four different conditions: the initially pure states with $v = 5$ ($---$) and $v = -5$ (\cdots) and the corresponding mixed states as (squares) and (xxx), respectively. For comparison, the LS case with $v = 5$, is also presented ($---$). The inset in (d) is for the SDS case with the initially mixed state for $v = 5$ (squares) with enlarged ordinate which reveals that it oscillates in tune with the LS case with $v = 5$.

Fig. 6. The LS case with various v with $\Gamma = 1.6 \times 10^{-4}$ for (a),(b) and with $\Gamma = 1.6 \times 10^{-3}$ for (c). In (a), ρ_{RR} vs. the rescaled time with $v = 0$ (thick line), ± 3.9 ($-\cdot-$), ± 4 ($---$), and ± 5 ($-\cdot-\cdot-$). In (b) and (c), purity vs. the rescaled time with $v = 0$ (thick line), ± 3 ($\cdot\cdot\cdot$), ± 3.9 ($-\cdot-$), ± 4 ($---$), ± 5 ($-\cdot-\cdot-$), and ± 10 (thin line). Note that the case with $v = \pm 10$ overlaps with the $v = 0$ case.

Fig. 7. Time evolution of (a) purity and (b) population with $\Gamma = 1.6 \times 10^{-2}$, for the LS case, at $v = 0$ (thick line), ($\cdot\cdot\cdot$), ± 3.9 ($-\cdot-$), ± 4 ($---$), ± 5 ($-\cdot-\cdot-$) and ± 10 (thin line).

Fig. 8. Upper panel: ρ_{RR} vs. the rescaled time. Lower panel: Purity vs. time. Here the LS case with $v = +5$ is presented at $\Gamma = 0$ (thick line), 1.6×10^{-4} ($---$), 1.6×10^{-3} ($\cdot\cdot\cdot$), and 1.6×10^{-2} ($-\cdot-$).

Fig. 9. ρ_{RR} vs. the rescaled time in (a) and (c). Purity vs. the rescaled time in (b) and (d). The SDS case with $\Gamma = 1.6 \times 10^{-3}$ is presented. For (a) and (b), $v > 0$: $v = 0$ (thick line), 2 ($---$), 3 ($\cdot\cdot\cdot$), 5($-\cdot-\cdot-$), and 10 (thin line). For (c) and (d), $v < 0$: $v = 0$ (thick line), -2 ($---$), -3 ($\cdot\cdot\cdot$), -5($-\cdot-\cdot-$), and -10 (thin line). Note the difference in the scale of ordinate in panels (a) and (c).

Fig. 10. ρ_{RR} vs. the rescaled time in (a) and (c). Purity vs. the rescaled time in (b) and (d). The WDS case with $\Gamma = 1.6 \times 10^{-3}$ is presented. For (a) and (b), $v > 0$; $v = 0$ (thick line), 2 ($---$), 3 ($\cdot\cdot\cdot$), 5($-\cdot-\cdot-$), and 10 (thin line). For (c) and (d), $v < 0$; $v = 0$ (thick line), -2 ($---$), -3 ($\cdot\cdot\cdot$), -5($-\cdot-\cdot-$), and -10 (thin line).

Fig. 11. ρ_{RR} vs. the rescaled time in (a) and (c). Purity vs. the rescaled time in (b) and (d). The WDS case with $v = 5$ is chosen for (a) and (b) and the WDS case with $v = -5$ is chosen for (c) and (d). $\Gamma = 0$ (thick line), 1.6×10^{-4} ($---$), 1.6×10^{-3} ($\cdot\cdot\cdot$), and 1.6×10^{-2} ($-\cdot-$). In panels (a) and (b) the $\Gamma = 0$ and $\Gamma = 1.6 \times 10^{-4}$ curves overlap to the extent that they cannot be distinguished.

Fig. 12. ρ_{RR} vs. the rescaled time in (a) and (c). Purity vs. the rescaled time in (b) and (d). The SDS case with $v = 5$ is chosen for (a) and (b) and the SDS case with $v = -5$ is chosen for (c) and (d). $\Gamma = 0$ (thick line), 1.6×10^{-4} ($---$), 1.6×10^{-3} ($\cdot\cdot\cdot$), and 1.6×10^{-2}

(- · -). Note the difference in the scale of ordinate in panels (a) and (c).

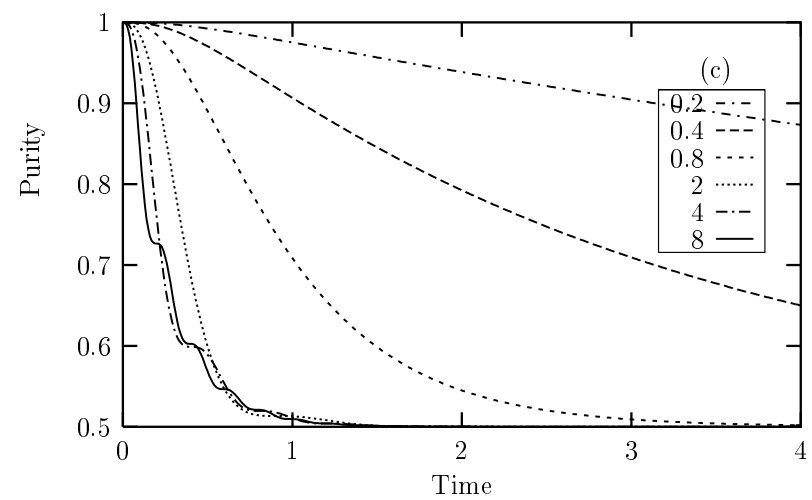
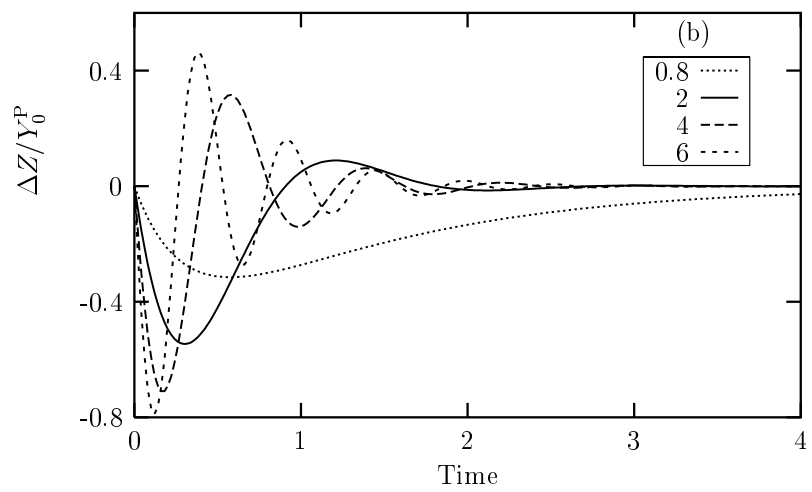
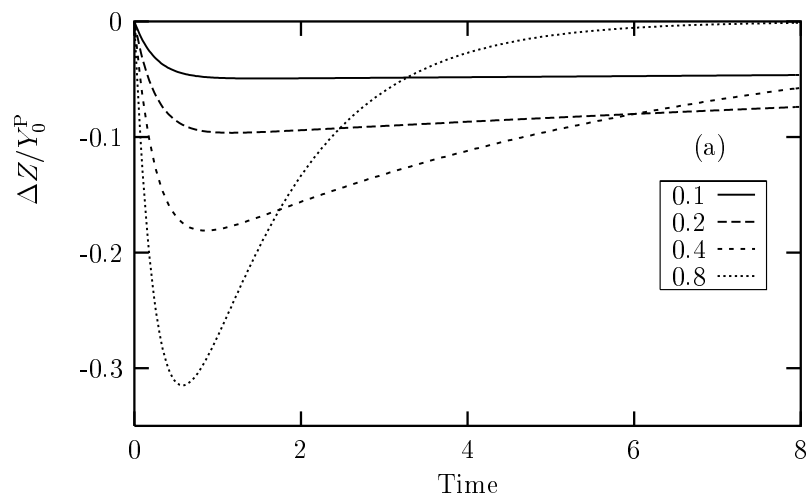


FIG. 1:
32

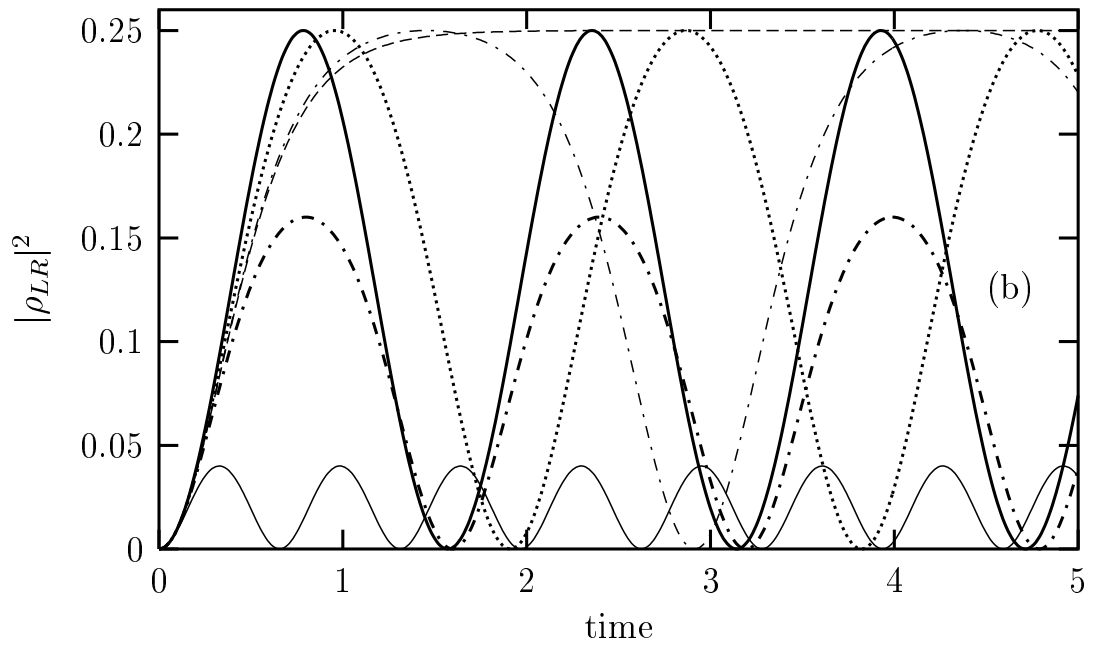
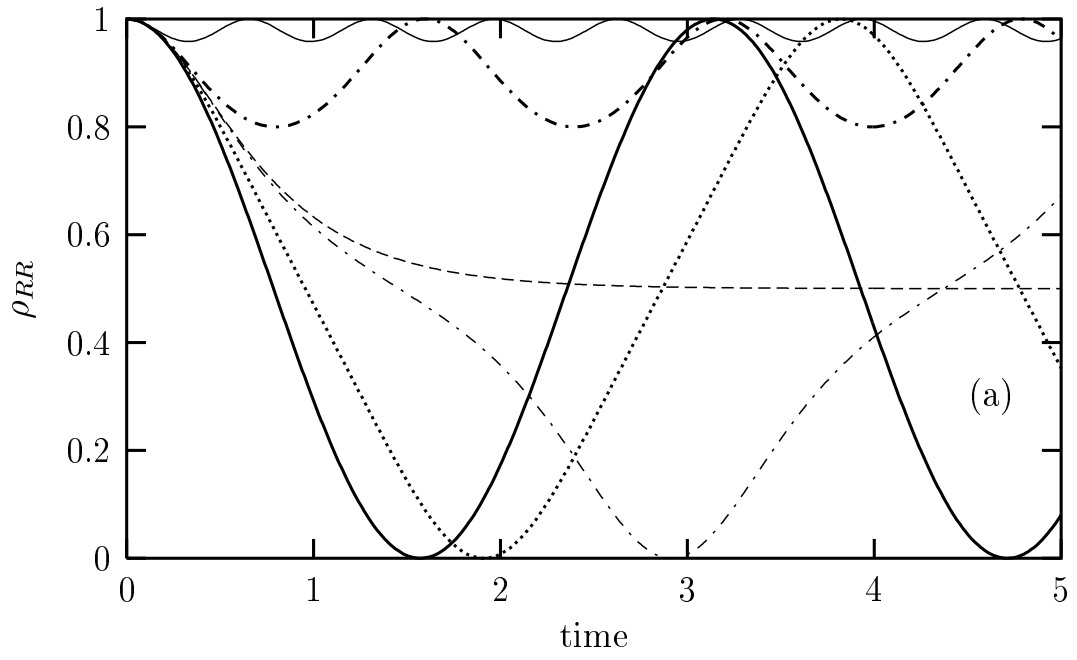


FIG. 2:

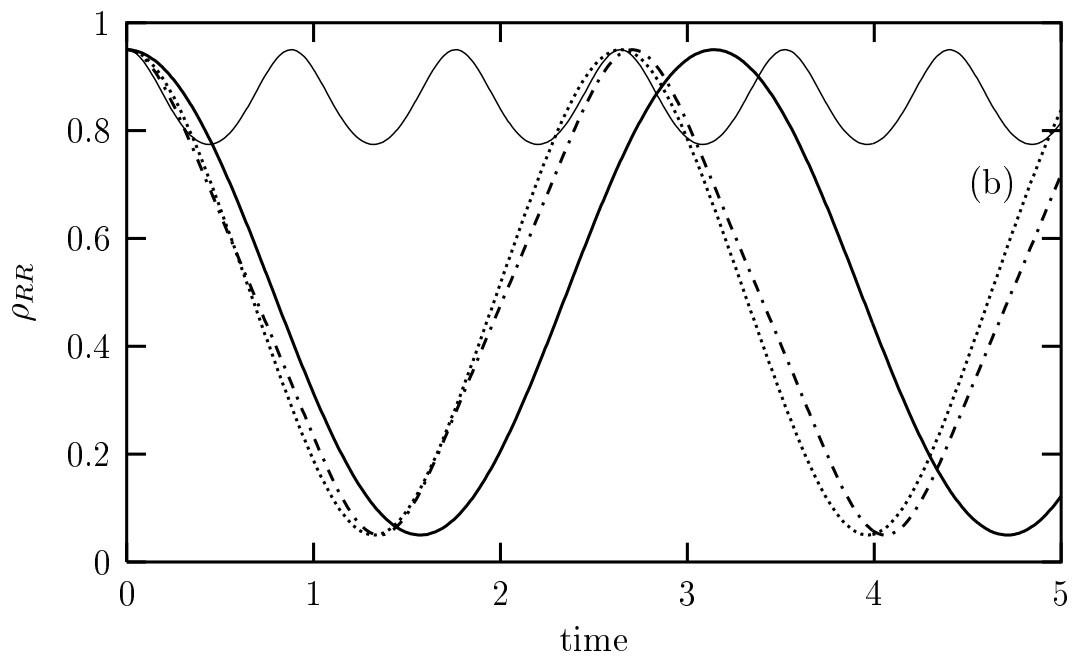
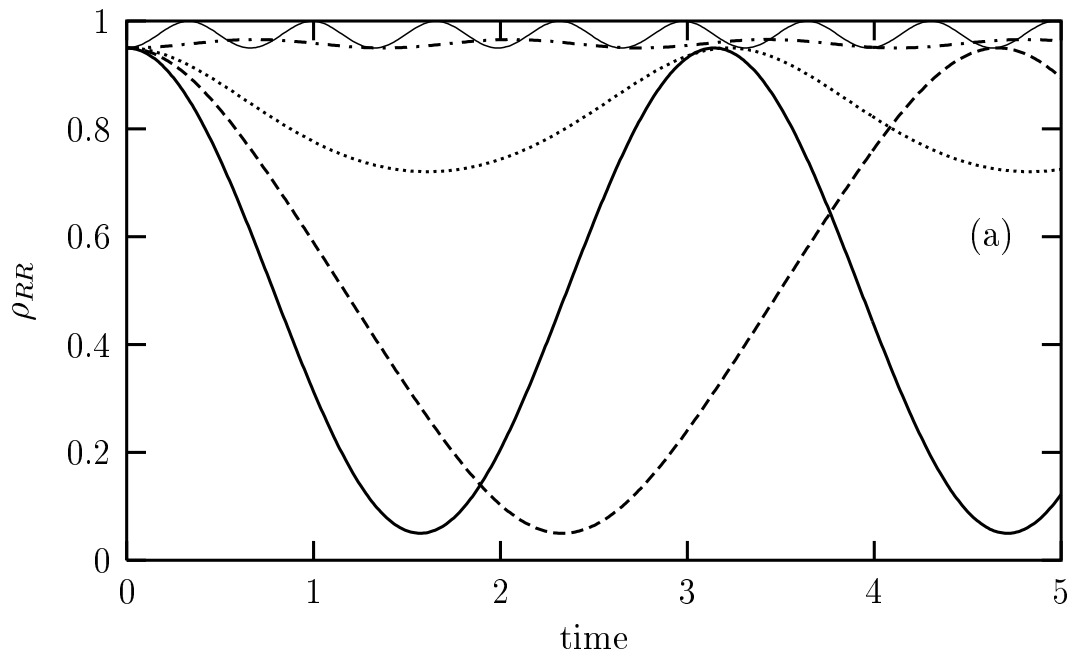


FIG. 3:

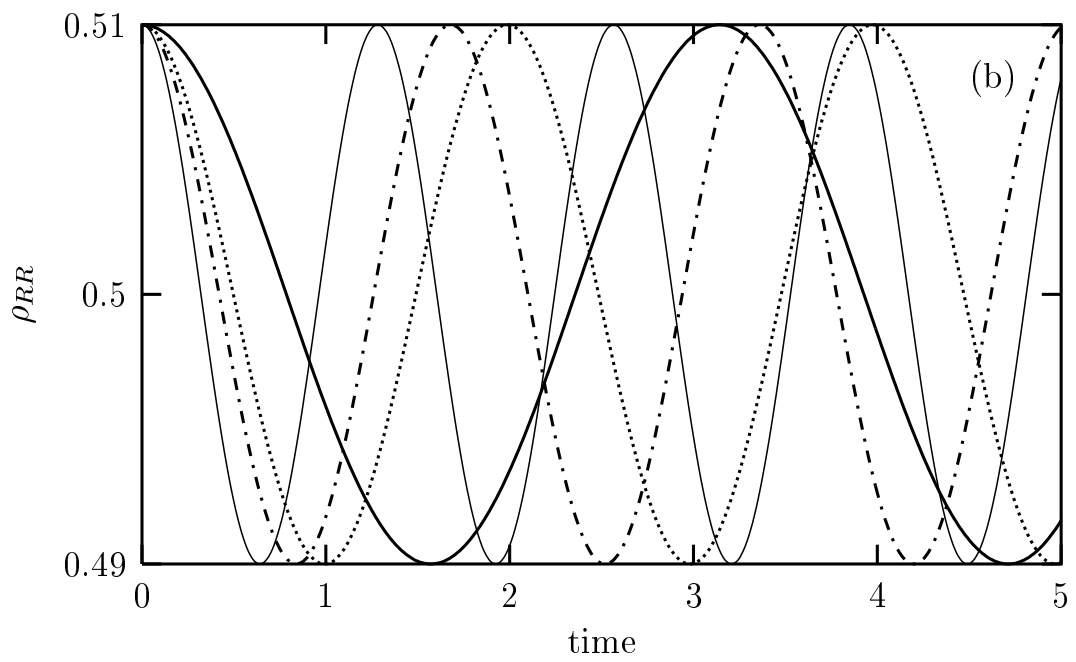
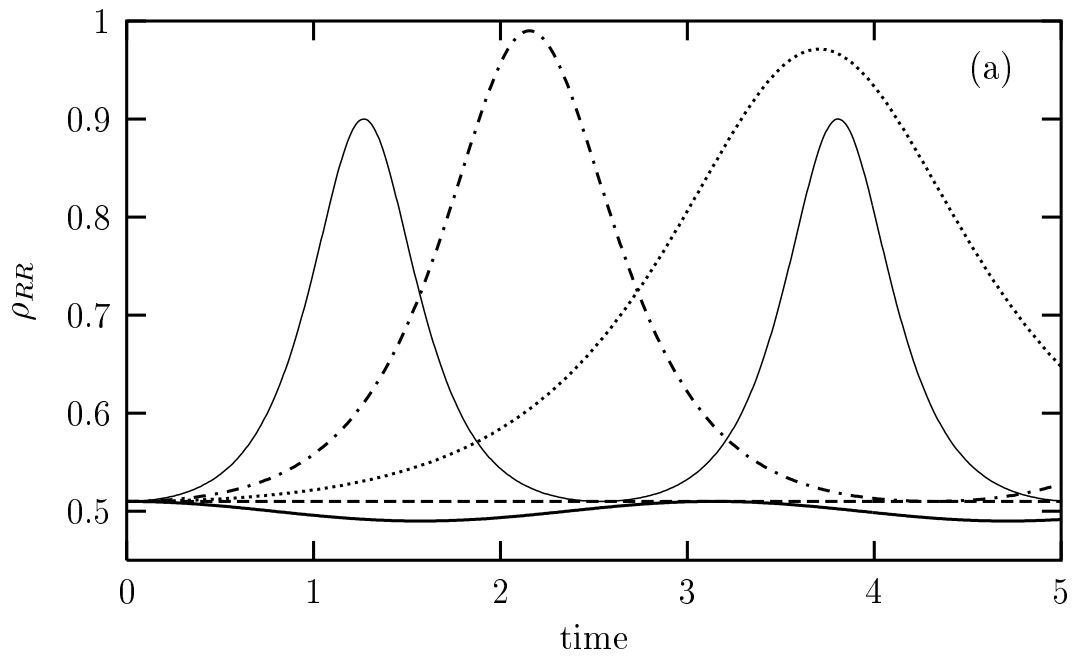


FIG. 4:

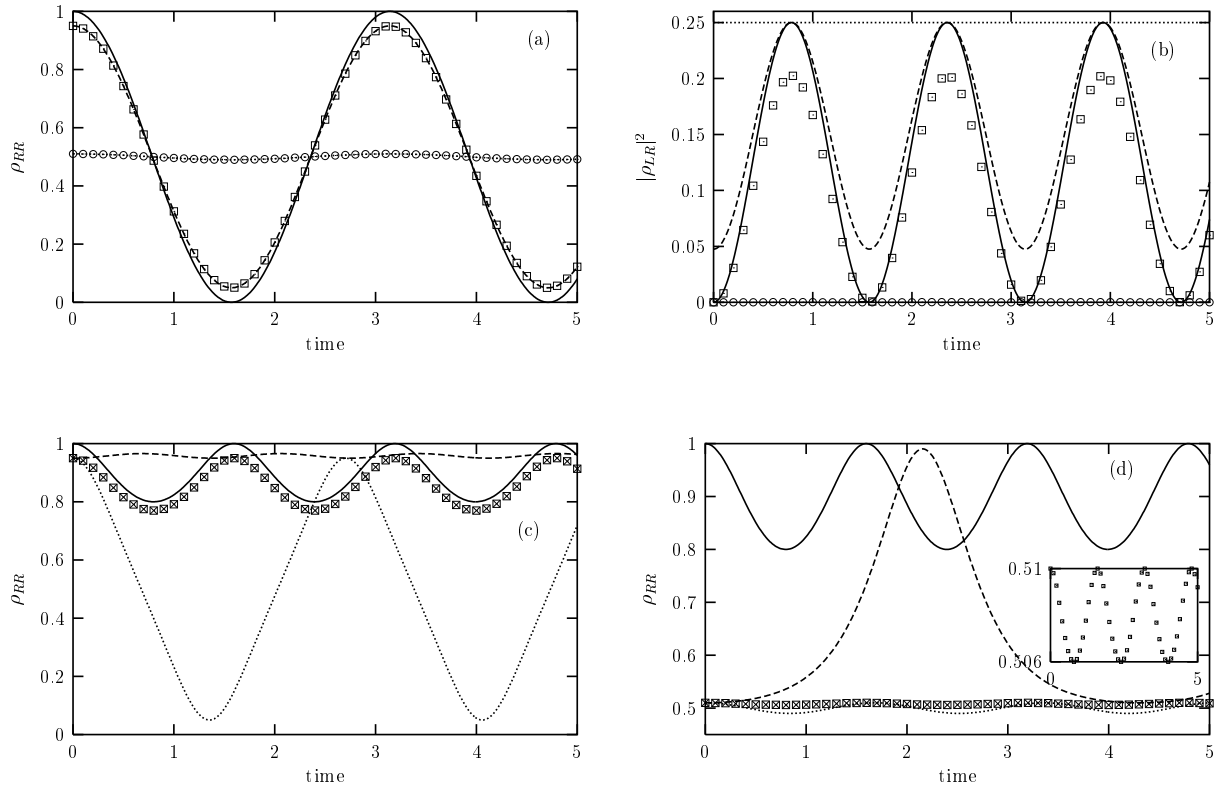


FIG. 5:

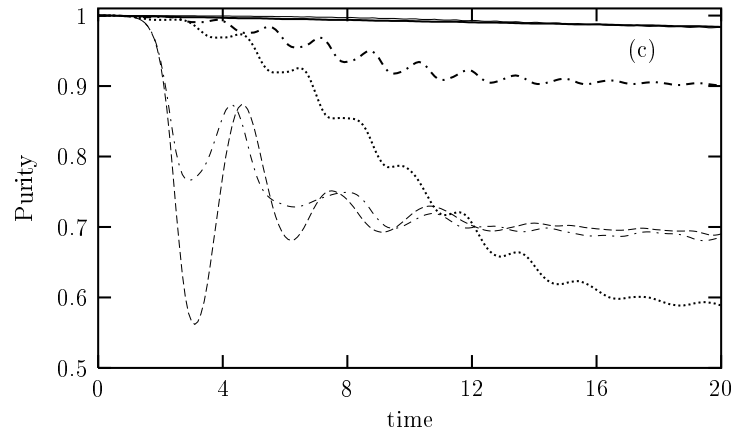
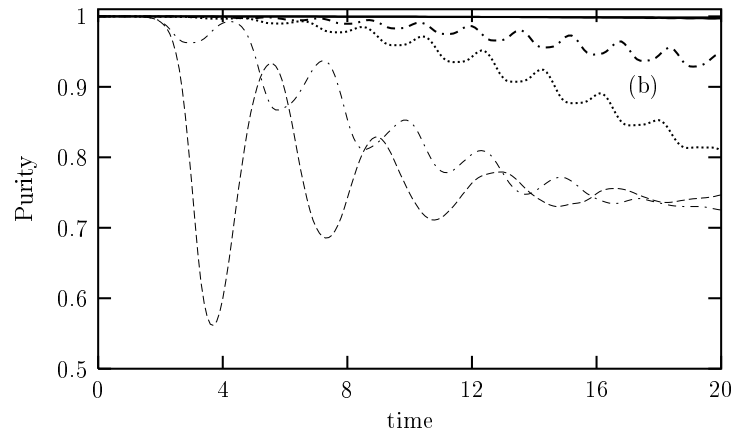
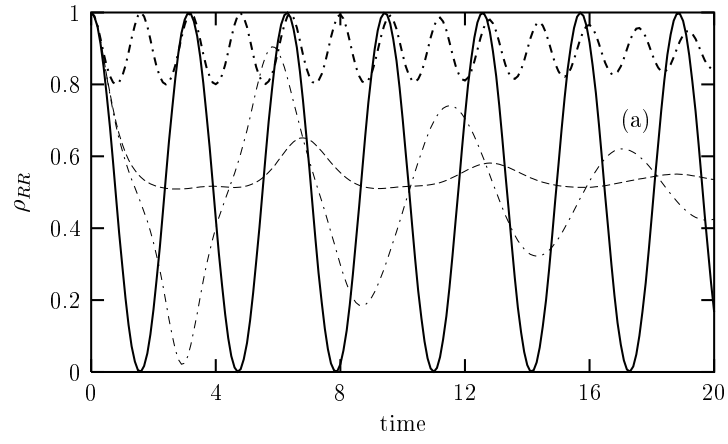


FIG. 6:

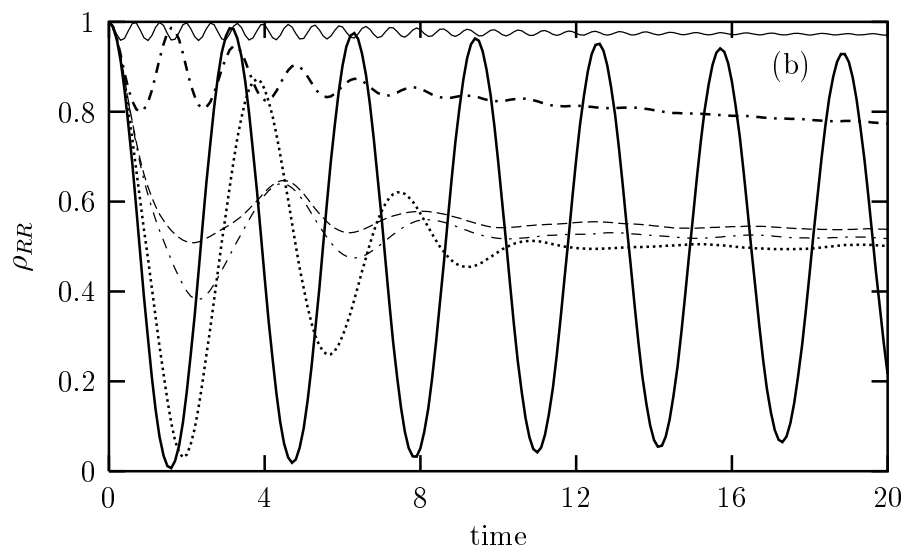
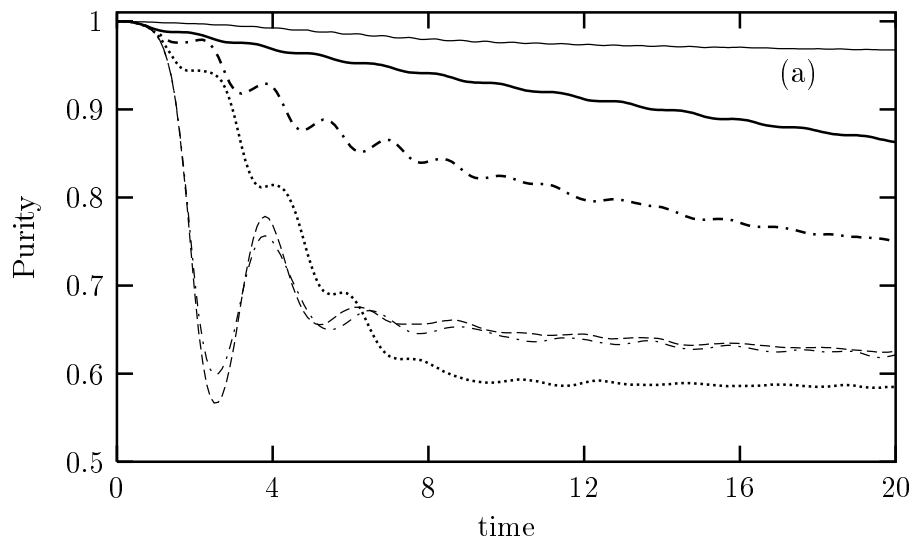


FIG. 7:

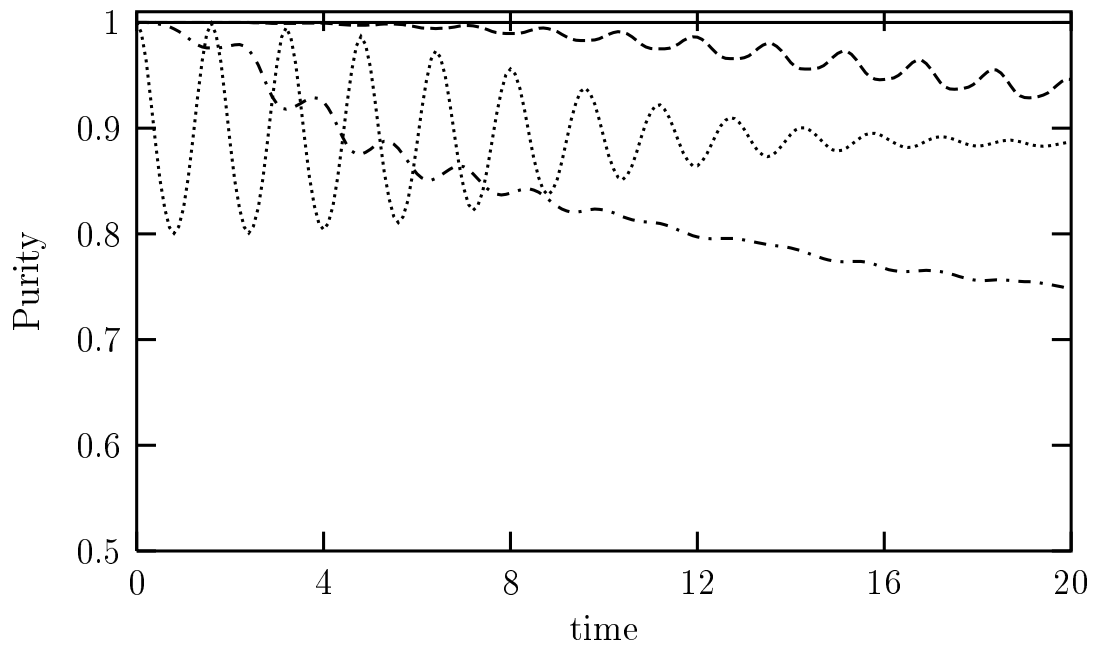
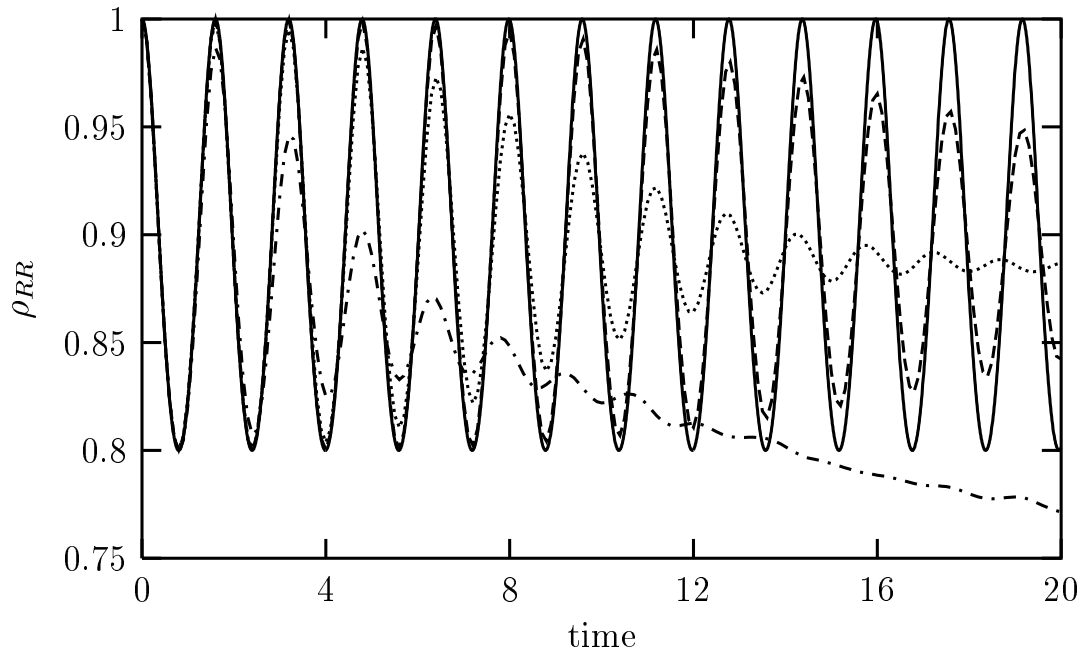


FIG. 8:

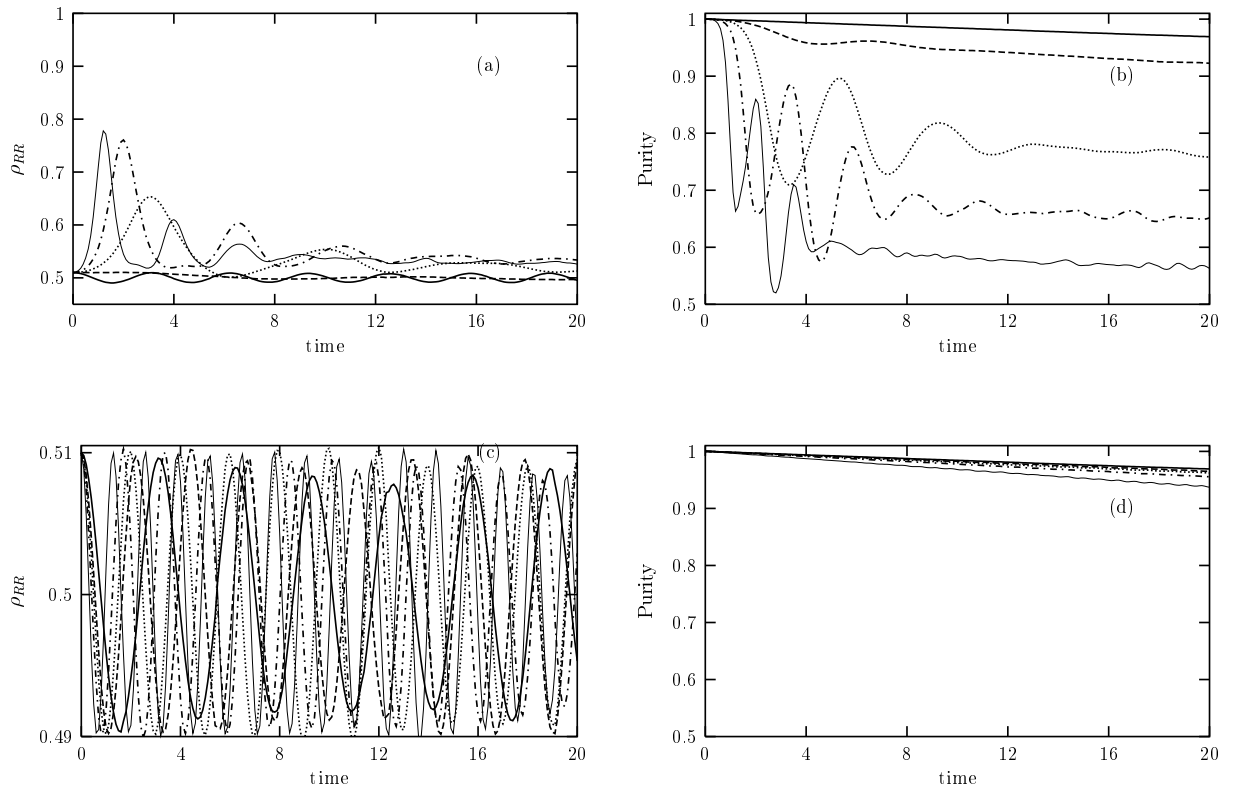


FIG. 9:

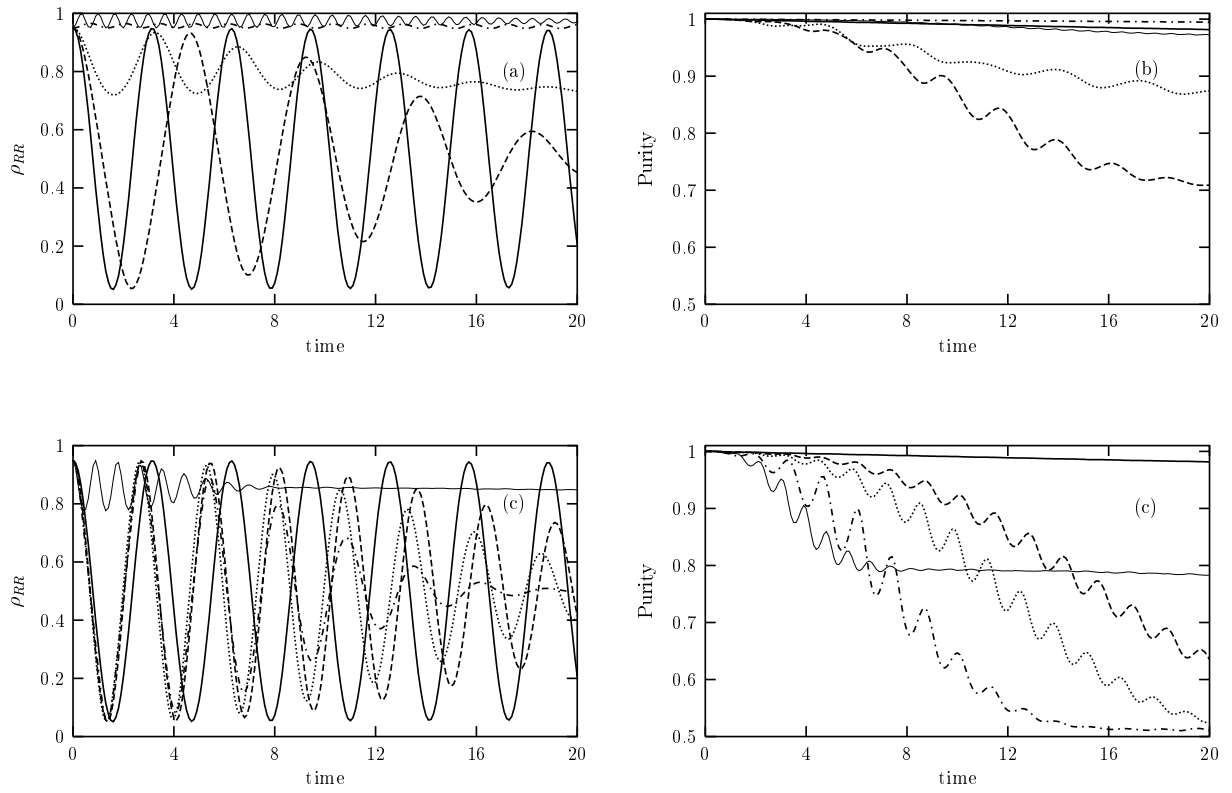


FIG. 10:

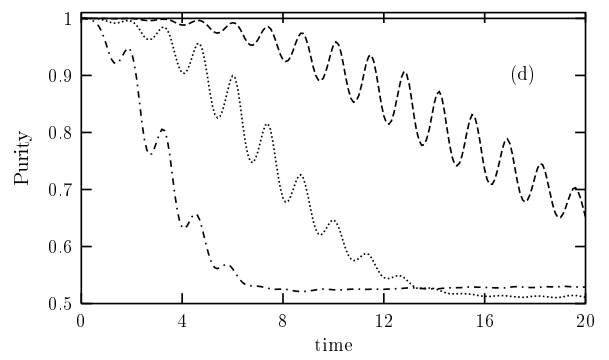
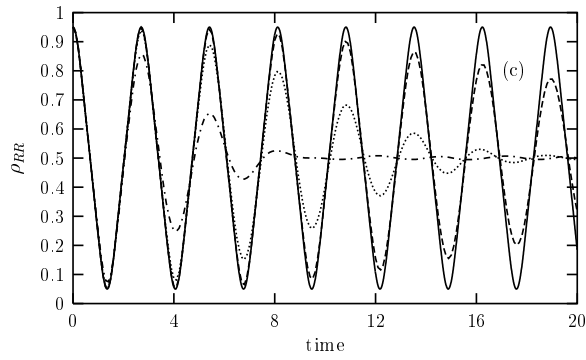
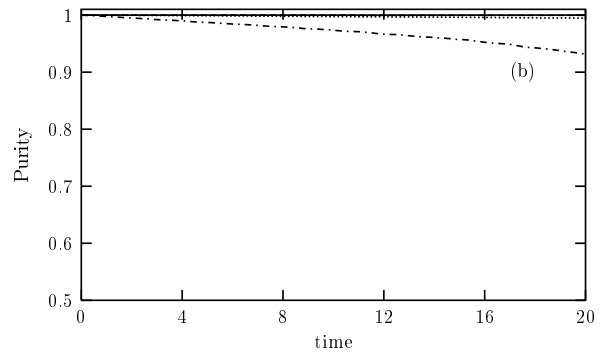
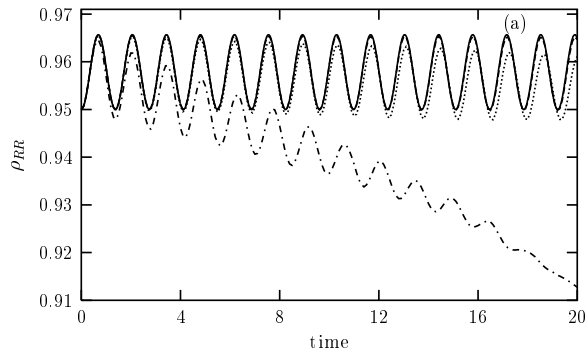


FIG. 11:

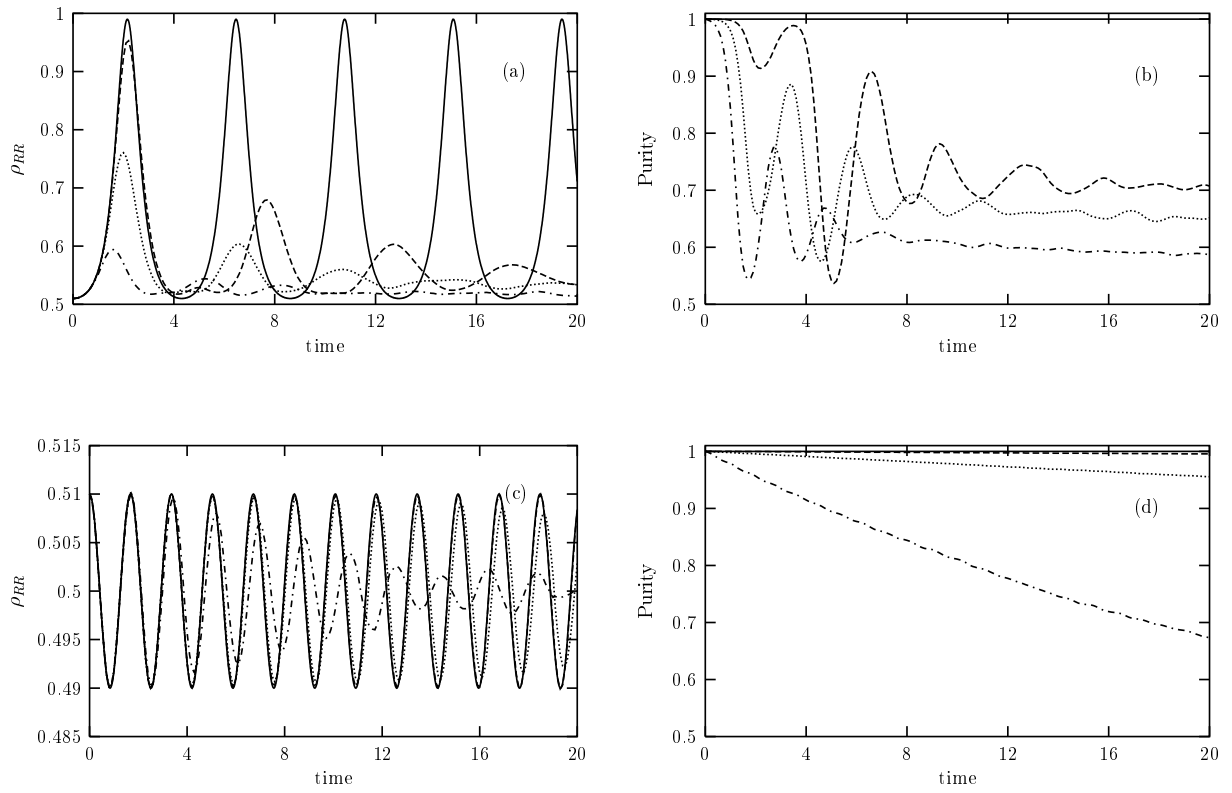


FIG. 12: